SAR simulations with SEMCAD,

a new FDTD software package for computational electrodynamics

Master Thesis by

Marie Fransson

In co-operation with Moteco AB, November 2001

Supervisors:

Anders Sunesson, Moteco AB, Lund

Anders Karlsson, Department of Electroscience, Lund

Abstract

A new software package for computational electromagnetics, SEMCAD, has been developed by Schmid & Partner Engineering AG in Switzerland. One special feature of this software package is the ability to compute SAR. SAR is a value corresponding to the power absorbed by the human tissue while exposed to microwave radiation. For antenna designers and cellular phone companies, this value is limited and consequently it is an important parameter in the antenna design process. In this master thesis the software is evaluated for SAR computations and compared with real measurements.

En ny programvara för elektromagnetiska simuleringar, SEMCAD, har utvecklats av Schmid & Partner Engineering AG i Schweiz. Det nya med programmet är att det även kan simulera SAR, strålningen som absorberas av huvudet. För mobiltelefontillverkarna finns det gränsvärden för SAR och därför är SAR en viktig parameter i antenndesignprocessen. I detta examensarbete är programvaran testad och de simulerade resultaten har jämförts med uppmätta resultat.

Acknowledgements

First, I would like to thank my supervisor Anders Sunesson at Moteco for all the support and for encouraging me while doing this master thesis. I will also like to thank my supervisor Anders Karlsson at the Department of Electroscience in Lund.

Moreover I would like to thank all the staff at Moteco and gigaAnt in Lund for everything. A special thanks to Peter Sjöblom and Björn Cederberg for all their support and all interesting discussions we have had during the master course. Thanks to Filip Lindau for help with IE3D and to Ola Carmonius for help with Pro/ENGINEER.

Furthermore, thanks to Harald Songoro and the staff at SEMCAD support for help with problems concerning the program.

Finally, thanks to Erik for his support and help with English spelling and grammar.

Table of contents

1 Introduction

In this Master Thesis, a new software package for electromagnetic simulations is examined. The name of this software is SEMCAD – Simulation platform for EMC, Antenna design and Dosimetry. The software is developed by a Swiss company named Schmid & Partner Engineering AG in co-operation with different universities in Switzerland. The software was released on the market in January 2001. The second version, 1.2, was released in May 2001 and version 1.4 is due in the end of November 2001. The numerical method used by the program is the Finite Difference Time Domain method (FDTD). This is the best method for simulating biological tissue. For more about this method see chapter 2.2.

A new feature of the program is the ability to make SAR computations. The SAR value is an important parameter for the antenna designer, describing how much power absorbed by human tissue. For electromagnetic radiators, there are threshold values for the maximum amount of power absorbed in different parts of the body. If those limits are exceeded, the antenna or the whole cellular phone has to be redesigned. More regarding SAR and the limits is found in chapter 2.3, also study chapter 7 for a discussion regarding SAR. The program uses models for human tissue as a head or a whole body.

The first object of this work was to learn how the program worked and try to do simple simulations. Then, simulations of different types of cellular telephones were done with different antennas, for example dipole antennas, quarter-wave stub antennas, patch antennas and helical antennas. These antennas are the most frequently used cellular phone antennas. For more information about the different types of antennas, see chapter 2.4. Instructions, how to run a simulation and things to consider when running a simulation are examined in chapter 3. An example of a simulation for a helical antenna is given in chapter 4, where also the different simulated results are presented and problems concerning the grid size are examined. Chapter 3 and 4 may thus be seen as a guide of the program.

Real SAR measurements are made on the DASY3 measurement system. This system measures the SAR value when the phone is communicating with a local base station. A parametrical study is done of how the SAR value changes when the phone is moved back and forth perpendicular to the head near the ear. In the program, there are predefined reference points at the ears where to place the phone, but the corresponding point on the phone is not predefined. This point is where the loudspeaker is placed, but an approximated box or groundplane contains no loudspeakers. A real phone is used and the position is changed to see what happens when the phone is moved from the predefined position. These measurements are compared with simulations in order to see how well the measurements correlates with simulations; see chapter 5.

A phone is studied with different antenna types, both in simulations and measurements. The difference in SAR value between a half-wave antenna and a quarter-wave antenna is studied, see chapter 6. Also, a patch antenna is simulated for 2.4 GHz and a dual band patch is simulated for both 900 MHz and 1.8 GHz. By the end of chapter 6, a real project from a CAD software package is simulated and measured.

The main subject of this report is the feature of the program that calculates SAR; more investigations on how an antenna can be modelled in SEMCAD, can be done in future work. SEMCAD has nice colour features. Unfortunately this thesis cannot be printed in colours. If you are interested in looking at colour plots, please contact the author. The computer used in the simulations in this thesis is a Pentium 3, 800 MHz with 512 MB RAM.

2 Theory and method

This chapter contains a description of the theory used in this thesis. First Maxwell's equations are described, then the FDTD method and the importance of numerical stability is explained. In chapter 2.3, the SAR value is examined and in the last chapter, the antennas used in cellular phones are explained and evaluated.

2.1 Fundamental theory of electromagnetics

The electromagnetic theory is based on four equations well known as Maxwell's equations. They were published by James Clark Maxwell (1831-1879) in 1864. In differential form the equations are:

$$\nabla \times E = -\frac{\partial B}{\partial t} \quad \text{Faraday's law} \quad (2.1)$$

$$\nabla \times H = J + \frac{\partial D}{\partial t} \quad \text{Ampère's law} \quad (2.2)$$

$$\nabla \cdot B = 0 \quad (2.3)$$

$$\nabla \cdot D = \rho \quad \text{Gauss law} \quad (2.4)$$

where

E is the electric field intensity [V/m]
H is the magnetic field intensity [A/m]
B is the magnetic flux density [Vs/m^2]
D is the electric flux density [As/m^2]
J is the free volume current density [A/m^2]
ρ is the free volume charge density [As/m^3].

The B-field and the D-field are coupled to the E-field and the H-field by the constitutive relations:

$$D = \varepsilon_0 \varepsilon_r E \quad (2.5)$$

$$B = \mu_0 \mu_r H, \quad (2.6)$$

where

ε_0 is the electric permittivity in free space [As/Vm]
ε_r is the relative electric permittivity in the material
μ_0 is the magnetic permeability in free space [Vs/Am]
μ_r is the relative magnetic permeability in the material.

The free volume current density can be expressed in terms of E-field with help of Ohm's law:

$$J = \sigma E, \quad (2.7)$$

where σ [A/Vm] is the conductivity of the material.

The free space around a radiating object can be divided into three regions. They are defined as:

$$0 < r < 0{,}62\sqrt{\frac{d^3}{\lambda}} \quad \text{Reactive near field region} \quad (2.8)$$

$$0{,}62\sqrt{\frac{d^3}{\lambda}} < r < \frac{2d^2}{\lambda} \quad \text{Near field region} \quad (2.9)$$

$$\frac{2d^2}{\lambda} \leq r \quad \text{Far field region} \quad (2.10)$$

where r is the distance from the source to the actual point, d is the diameter of the radiating object and λ is the wavelength in free space. For small antennas there are more restrictions on how the far field region is defined: $r \geq 10\lambda$ and $r \geq 10d$. In the reactive near field region, the imaginary part of the electric field, i.e. the stored energy, is large compared to the energy radiating from the object. In the near field region, the imaginary and real parts of the electric field are small. In the far field region the imaginary part is zero and the electric field is propagating as a spherical wave.

For more information about fundamental electromagnetics, see [1] and [2].

2.2 The Finite Difference Time Domain method

The Finite Difference Time Domain (FDTD) method is a numerical method for solving partial differential equations in both time and space. The method has been known for a long time, however not commonly used until the beginning of the 1980's, as a lot of computer memory is needed for the implementation of the method.

2.2.1 FDTD description of Maxwell's equations

Kane S. Yee presented the method in a paper in 1966 [3]. He introduced a special scheme of discretising space. He described how the field components should be oriented in a cell, see figure 2.1. This means that each one of the three E-field components is surrounded by two H-components, all oriented perpendicular to the E-field.

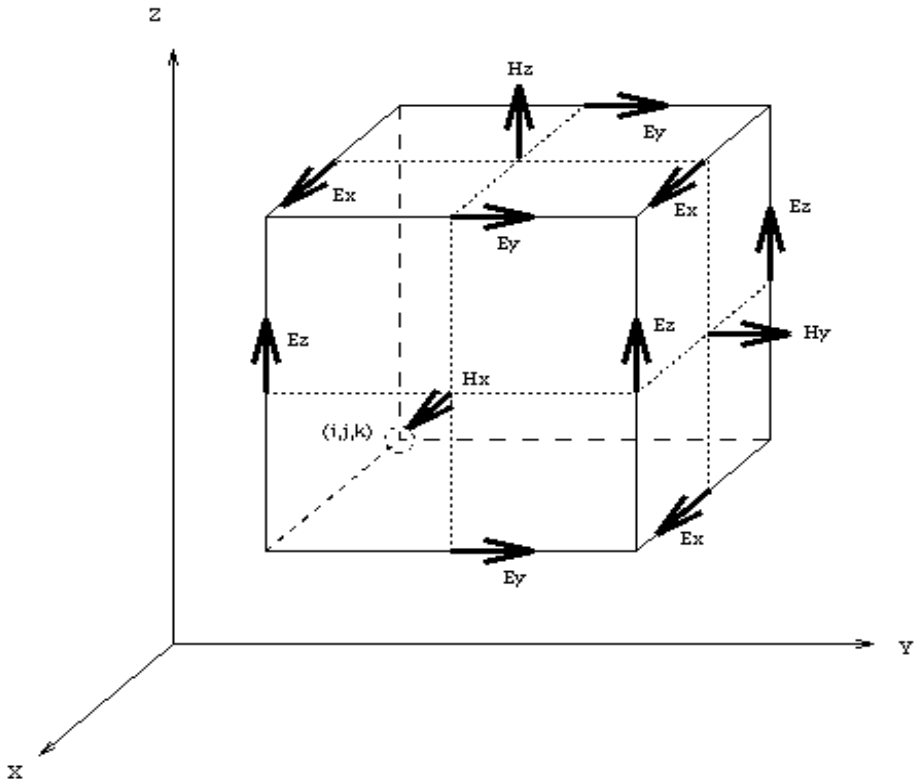

Figure 2.1, The Yee cell

The method is based on a second order finite-difference approximation of the partial derivatives in Maxwell's equations. The solution is a direct solution of Maxwell's equations and not of Helmholtz's equation, which is commonly used when solving this kind of problems. The first two of Maxwell's equations are solved at the same time for the E and the H-field. This gives unique stability to the method. The E and H-field components are updated in a leap-frog scheme using the finite-difference form of Maxwell's curl equations (2.1) and (2.2).

The first partial space and time derivatives can be written as:

$$\frac{\partial F(i,j,k,n)}{\partial x} = \frac{F^n(i+1/2,j,k) - F^n(i-1/2,j,k)}{\Delta x} + \mathrm{O}\left[(\Delta x)^2\right] \qquad (2.11)$$

$$\frac{\partial F(i,j,k,n)}{\partial t} = \frac{F^{n+1/2}(i,j,k) - F^{n-1/2}(i,j,k)}{\Delta t} + \mathrm{O}\left[(\Delta t)^2\right], \qquad (2.12)$$

where F can be either E or H at time n·Δt. The variables i, j, k are the indices of the space lattice, and $\mathrm{O}[(\Delta x)^2]$ and $\mathrm{O}[(\Delta t)^2]$ are the error terms. The equation (2.11) is applied to Maxwell's curl equations (2.1) and (2.2) and leads to the following equations for the E_x component:

$$\frac{\mathrm{E_x}\big|_{i,j,k}^{n+1} - \mathrm{E_x}\big|_{i,j,k}^{n}}{\Delta \mathrm{t}} = \frac{1}{\varepsilon_{i,j,k}}\left(\frac{\mathrm{H_z}\big|_{i,j+1/2,k}^{n+1/2} - \mathrm{H_z}\big|_{i,j-1/2,k}^{n+1/2}}{\Delta y} - \frac{\mathrm{H_y}\big|_{i,j,k+1/2}^{n+1/2} - \mathrm{H_y}\big|_{i,j,k-1/2}^{n+1/2}}{\Delta \mathrm{z}} - \sigma_{i,j,k}\,\mathrm{E_x}\big|_{i,j,k}^{n+1/2}\right) \qquad (2.13)$$

Assuming the approximation:

$$\mathrm{E_x}\big|_{i,j,k}^{n+1/2} = \frac{\mathrm{E_x}\big|_{i,j,k}^{n+1} - \mathrm{E_x}\big|_{i,j,k}^{n}}{2} \qquad (2.14)$$

the equation (2.13) can be reduced to (2.15):

$$\mathrm{E_x}\big|_{i,j,k}^{n+1} = \left(\frac{1 - \frac{\Delta t \cdot \sigma_{i,j,k}}{2 \cdot \varepsilon_{i,j,k}}}{1 + \frac{\Delta t \cdot \sigma_{i,j,k}}{2 \cdot \varepsilon_{i,j,k}}}\right)\mathrm{E_x}\big|_{i,j,k}^{n} + \left(\frac{\frac{\Delta t}{\varepsilon_{i,j,k}}}{1 + \frac{\Delta t \cdot \sigma_{i,j,k}}{\varepsilon_{i,j,k}}}\right) * \left(\frac{\mathrm{H_z}\big|_{i,j+1/2,k}^{n+1/2} - \mathrm{H_z}\big|_{i,j-1/2,k}^{n+1/2}}{\Delta y} - \frac{\mathrm{H_y}\big|_{i,j,k+1/2}^{n+1/2} - \mathrm{H_y}\big|_{i,j,k-1/2}^{n+1/2}}{\Delta \mathrm{z}}\right) \qquad (2.15)$$

The corresponding equations for the other components (E_y, E_z, H_x, H_y, H_z) can be written analogously. This leads to six equations for each cube in the lattice.

The main idea of how the computation is performed, called leap-frog computation, is as follows; in the first timeslot (n), the E-field is calculated, and at n+1/2 the H-field is calculated, and again at n+1 the E-field is updated from n. Then the computation continues until it has run through all the time steps.

2.2.2 Numerical stability and dispersion

Numerical stability always needs to be considered when using numerical methods. When setting up the grid, the cells have to be sufficiently small compared to the wavelength and the size of the objects, otherwise phenomena like aliasing and diverging simulation can occur.

The FDTD method divides space into a lattice of Yee cells. The cells can be equidistant, figure 2.2, or non-equidistant, figure 2.3. This gives the advantage that the cells can be concentrated on an interesting area, where for example the structure is complex, without degrading the calculations more than necessary. Sub-grids can be used too, figure 2.4, when some cells are divided into new cells. This saves a lot of computational time.

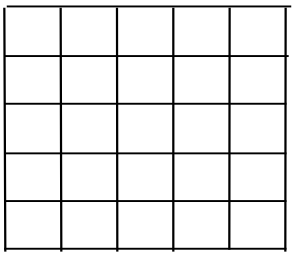

Figure 2.2, An example of equidistant grids

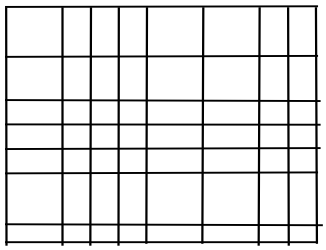

Figure 2.3, An example of non-equidistant grids

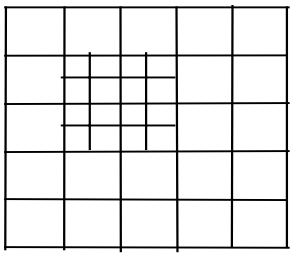

Figure 2.4, An example of sub-grids

To yield numerical stability the time step for the updating process has to be limited compared to the Courant-Freidrich-Levy criterion. For a more comprehensive presentation of CFL, see [4] page 87ff. The authors of the article states that for the FDTD formulation of Maxwell's equations, this criterion is:

$$\Delta t \leq \frac{1}{c\sqrt{\frac{1}{(\Delta x)^2}+\frac{1}{(\Delta y)^2}+\frac{1}{(\Delta z)^2}}} \qquad (2.16)$$

where Δx, Δy, Δz are the differences in space and c is the speed of light in the material of the current cell. From equation (2.16), it is clear that the simulation time step has a large impact on the results of the simulation. For a non-equidistant cell grid the smallest cell size has to be considered so that the Courant-Freidrich-Levy criteria is fulfilled for this cell. As a result, when using small cells, this gives long simulation times.

In all simulations of the three-dimensional Maxwell equations, wave propagation suffers from numerical dispersion. This means that the analytical phase velocity differs from the simulated. The numerical dispersion depends on the frequency and the direction of propagation of the wave. The numerical dispersion is inherent in FDTD and has to be kept as small as possible. This can be achieved by reducing the grid size. A cell size of 1/10 of the wavelength is recommended in order to avoid numerical dispersion.

2.2.3 Different types of boundary conditions

Unfortunately it is not possible to simulate an infinite space. Computers cannot store an unlimited amount of data; consequently the computation domain has to be limited in size, and boundary conditions has to be used. The outer cells are supposed to simulate infinity regarding to the object.

There are two types of boundary conditions, one in time and one in space. The time boundary conditions are for example initial values of the fields, and are not used here since the field is always set to zero before the computational time has started. The source is turned on the moment the simulation starts. A voltage gap is introduced between two cells and this is how the excitation is done in FDTD. The space boundary conditions are the conditions at the object surfaces of the objects and at the outer limit of the computational area.

There are two kinds of conditions for the cells that borders to infinity; the ABC and the RBC. When using the RBC – radiation boundary condition – all the energy in the outer cells is radiating outside the grid. When using the ABC – absorbing boundary conditions – the field is not radiating back into the adjacent cells, the final

cells absorb all the energy. The error using these approximations should theoretically be 0.1 % for both methods. However, the error is often larger, since the wave can contain different frequencies and may come from any direction compared to the cell.

There are many possible boundary conditions in the FDTD method that can be used for the outer cells. The three most frequently used are Mur, Highdon (both named after their inventor) and PML – perfectly matched layers. They are all three examples of ABC. These conditions are not essential for this thesis; the interested reader can find more information on the subject in [4] page 158ff.

The boundary conditions for the objects are PEC – perfect electric conductor – and PMC – perfect magnetic conductor. This is for surfaces that are perfect conductors. Their boundary values of the E-field or the H-field are set to zero. Objects can also have dielectric boundary conditions and electrical parameters attached.

2.2.4 Advantages and disadvantages with FDTD

In FDTD, simulations can be computed for a spectrum of frequencies at the same time. This is done when simulating a gaussian sine signal containing a band of frequencies. It implies that the antenna parameters described in chapter 2.4 can be found as well as the resonance frequency of the antenna. Then a simulation for a specific frequency with a sine signal can be done. This type of simulation gives results in the frequency domain and they are the near and far fields for this specified frequency. This is necessary because the storage in the computer is not that large as needed if a time domain simulation is done with the same computational area.

Because of the way the grid generation is done in the FDTD method, the simulated object cannot be very complex; the complexity adds cells and time and this requires significant computer power. Approximations will be done when the grid is generated. The method has some difficulties modelling circular shapes such as cables, but it is certainly the best method for modelling biological heterogeneous tissues and, as in this case, to examine the SAR value. It allows an accurate description of the antenna and a simple model for complex scattering phenomena. It is not suitable for scattering problems of a large frequency range, even if it has been done; in that case it is better to use another numerical method such as ray tracing model or the method of moments. The FDTD method applied to electrodynamics is well described in the literature, [4] is recommended.

2.3 SAR – Specific Absorption Rate

SAR is a value describing how much power absorbed in biological tissue when the body is exposed to electromagnetic radiation. The mathematical definition is:

$$SAR = \frac{\sigma \cdot E^2}{\rho}, \qquad (2.17)$$

where E is the Electric field, σ is the conductivity and ρ is the density. SAR is measured in W/kg. SAR can be expressed in two ways; one way is to compute an average value of SAR in a cell of 1 gram and the other way is to compute an average value in a cell of 10 grams. Of course, SAR can be measured over a whole body, but with the power levels in cellular phones, 2 W, the SAR value averaged over a whole body would be hardly measurable. The interesting areas are the head and the brain tissue. SAR is important in the antenna design process since the value is restricted and it is not to be exceeded.

In Sweden and the rest of Western Europe the maximum average value is set to 2 W/kg over 10 grams by the standardisation organisation European Committee for Electrotechnical Standardization, CENELEC. In the United States and many other countries the maximum average value is set to 1.6 W/kg over 1 gram by another standardisation organisation called FCC – the Federal Communications Commission. For a detailed discussion of SAR, see chapter 7. For a discussion of SAR measurements, see chapter 5.

2.4 Antennas for cellular phones

An antenna is a device for transmitting and/or receiving electromagnetic energy. It is the component between free space and a wave-guide. Antennas can be seen in two ways, either as an electrical component in an electric circuit or as a radiator in free space.

The performance of an antenna as a radiator is presented in a far field radiation pattern. From this pattern parameters such as gain and directivity can be derived. These two parameters are closely related. The gain is "the ratio of the power gain in a given direction to the power gain of a reference antenna in its referred direction", see [5] page 58. The directivity is "the ratio of the radiation intensity in a given direction from the antenna to the radiation intensity averaged over all directions", see [5] page 39.

When describing an antenna as an electric component, three useful parameters are used. The voltage reflection coefficient, Γ, is a measure of how much power that is reflected back into a feeding cable compared to how much power that is transmitted to the antenna. Γ is defined in the range $|\Gamma|\leq 1$ and is generally complex. If $|\Gamma|=1$, the circuit acts like an open circuit or a short circuit, hence all power is reflected. If $\Gamma=0$, all power is transmitted and the antenna is perfectly matched, to the transmission line.

From Γ, another interesting antenna parameter is defined and that is the standing wave ratio, SWR, sometimes called the voltage standing wave ratio, VSWR. SWR is a value describing the ratio of the maximum value to the minimum value of the electric field intensity of a standing wave.

$$SWR = \frac{|E_{\max}|}{|E_{\min}|} = \frac{1+|\Gamma|}{1-|\Gamma|}, \quad 1 \leq \text{SWR} < \infty. \qquad (2.18)$$

When SWR=1 no standing wave appears and all power is transmitted. If the SWR value is large the reflection coefficient is close to one and the antenna does not transmit any power.

For antenna designers the frequency bandwidth is important. Bandwidth can for example be defined as the band of frequencies for which the antenna has better SWR than 2.

Analogously with SWR, the return loss or S11 is used.

$$RL = S11 = -20\log|\Gamma| \qquad (2.19)$$

This parameter shows how much power that is reflected at a certain frequency. As seen in (2.19) the SWR value and the S11 value are the same, expressed in different ways. An SWR value of 2, corresponds to a return loss value of about –10 dB.

An antenna has a characteristic input impedance that can be complex. The absolute value of the input impedance should be as close to 50 Ω as possible, to fit standards for feed cables etc. If the antenna has another input impedance, matching components have to be used to obtain a 50 Ω impedance at the feed point. When the input impedance is 50 Ω, S11 is close to negative infinity and SWR is 1. Examples of

these three parameters are found in chapter 4 on the simulations of a helical antenna. For more information about antennas, see for example [5].

2.4.1 Dipole antennas

A dipole antenna has an easy structure and consists normally of just a metal wire (whip) with a specified length depending on the wavelength. A dipole antenna is easy to produce and therefore cheap compared to other antennas. These antennas were mainly used in the first types of cellular phones. The electrical feed point is in a cellular phone attached at the bottom of the antenna. Currents from the feed point moves along the metallic surface of the wire and introduce an outgoing electric field from the wire. The polarisation of the radiated field is linear and parallel to the antenna axis. The antenna can be made smaller with surrounding plastics to increase the dielectric constant.

The first antenna used in a cellular phone was a half-wave dipole antenna. Then a monopole was used with a length of a quarter-wave. The half-wave antenna nowadays is used as an extensible antenna because of the disadvantage with always having a long wire outside the phone. The end-fed quarter-wave antenna has a theoretical input impedance of 36 Ω and an end-fed half-wave antenna has a theoretical impedance of 300 Ω. So when these antennas are used, there is sometimes a need to have matching components to obtain 50 Ω at the feed point. The radiation pattern looks like an apple and this is characteristic for a dipole antenna, see figure 2.5.

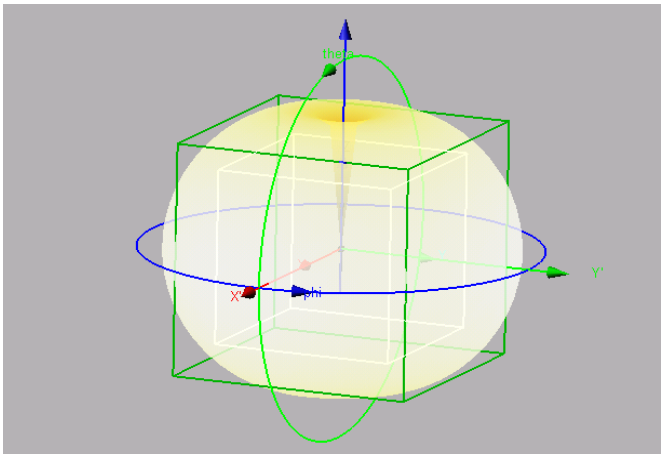

Figure 2.5, The radiation pattern from a dipole antenna

2.4.2 Helical antennas

A helical antenna is a mix between a loop antenna and a dipole antenna. The antenna has in most cases larger bandwidth than other antennas. The shape reminds of a spring, see figure 2.6.

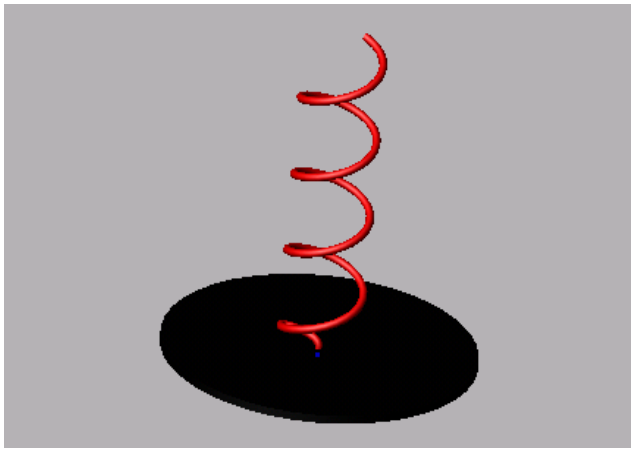
Figure 2.6, A helical antenna on a circular groundplane

A helical antenna can be used in two types of modes. One mode is the normal mode in which the far field radiation pattern in free space is similar to a dipole antenna pattern. The other way of using a helical antenna is in axial mode. Then the antenna will be more directive. The normal mode is used in mobile communications because the antenna has to have the same gain in all directions. All dimensions are small compared to the wavelength and the length of the wire is dependent on the desired type of helical antenna. A quarter-wave or a half-wave helical antenna is possible.

The characteristic impedance depends on the pitch angle for the antenna, the diameter and also on the thickness of the wire. A helical antenna does not always need matching because it is matched by altering the dimensions of the helical object, see [5] page 505.

2.4.3 Patch antennas

Patch antennas in cellular terminals are internal antennas. A metal patch plane is etched on a dielectric substrate and the substrate is put on a groundplane. In cellular terminals the whole terminal is used as groundplane. Commonly used shapes of a patch are circular, or rectangular, however it can have a very irregular shape and also have holes in it. The antenna is usually linearly polarised and the field lines are parallel to the long axis, but the antenna can also be made with circular polarisation. The substrate should have low losses; otherwise the power radiated by the antenna is not acceptable in the GSM system. This is even more important when using high frequencies. Simulations of different types of patch antennas are done in chapter 6.

The patch antenna can have different types of feed structures. The most common ones are fed with a microstrip line or a coaxial cable. The feed point is important and the characteristic impedance depends on it.

The antenna introduces a field in the substrate between the metallic patch and the groundplane; this field generates surface currents on the patch and these currents are the source of the outgoing fields. The groundplane has to be sufficiently large compared to the wavelength so that the currents on the groundplane is minimised. The bandwidth of the patch antenna depends on the thickness and the dielectric constant of the substrate. Usually the bandwidth is fairly small since the antenna cannot be thick enough. The disadvantage of this antenna is that it has problems with large radiated power levels and the polarisation is difficult to control. This makes the antenna difficult to use.

3 The SEMCAD program

This software is developed in Switzerland by Schmid & Partner Engineering AG in co-operation with different universities and institutes in Switzerland. It uses, as described in chapter 2.2, the FDTD method and its specialisation is the SAR computation. Electrical parameters of different body tissues, known as the Gabriel parameters, are included in the software package. They are research results from a Swiss university. [6]

The basic requirements for running this program with a computer are fulfilled by a modern PC. However, it takes a lot of time and memory to do simulations even with a high performance computer. The computer requirements depend on what type of simulation is desired, and the area size, time and complexity in the simulation.

3.1 Phantoms

SEMCAD has different phantoms available for simulations. The phantom that is most often used in this thesis is the SAM phantom. SAM (The Specific Anthropomorphic Mannequin) is a new model based on the 90th percentile dimensions of an adult male head based on an anthropomorphic study of US Army personnel, see figure 3.1. It compounds of two tissues, one shell of 2 mm to represent the skin and one homogenous liquid inside the shell to represent the brain tissue. This phantom will probably be the next measuring standard. Today, the standard phantom is the generic twin phantom, see figure 3.2. The generic twin phantom is based on an anthropomorphic study of 52 European persons. The shape around the ear corresponds to the 90th percentile of the data. It has two tissues, one skin and one homogenous liquid inside.

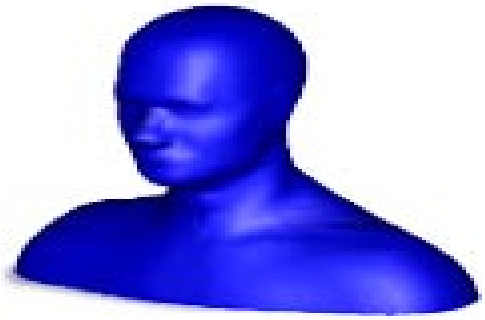

Figure 3.1, The SAM phantom

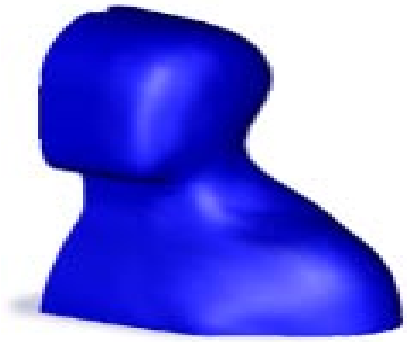

Figure 3.2, The generic twin phantom

These two models are both homogenous models. This means that the brain tissue is approximated with one dielectric constant and one electric loss constant. However, heterogeneous phantom models are available with many layers corresponding to each brain tissue with different electrical parameters. Of course it is easier to simulate a homogenous model. FDTD prefers models with less complex structure and a heterogeneous model would be very complex; the number of cells increases with complexity. The electrical parameters are different in the two homogeneous models depending on different standards and on the different shapes. The electrical parameters also change with frequency. The dielectric constant (permittivity) of the shell (ε_r=4.5) is the same for all frequencies. For the brain tissue the parameters varies as seen in table 3.1. The losses (conductivity) are higher for the SAM model than for the generic twin model; this means that the SAR value is generally 10 % higher in the

SAM model than in the generic twin model. However the differences also depend on the different shapes of the two models. See chapter 5.3 for the simulated differences for these phantoms.

For 900 MHz	ε_r	σ[A/Vm]
Generic twin	42.5	0.85
SAM	41.5	0.97
For 1800 MHz	ε_r	σ[A/Vm]
Generic twin	40.5	1.69
SAM	40.0	1.40

Table 3.1, Relative permittivity and conductivity for brain tissue, used in the two phantoms

3.2 A guide on how to run a simulation in SEMCAD

This is a practical guide on how to run a simulation in SEMCAD. This chapter should be read together with the SEMCAD reference guide or with the program running on a computer at the same time, otherwise this chapter can be hard to understand. The chapter is divided into three parts; one for the model, one for the simulations, and the last for the post-processing features.

3.2.1 Modelling in SEMCAD

Start a new window and select a new project name; what first appears is the modelling mode. First of all, the model units are chosen. A model unit defines the real distance in meters that corresponds to 1 unit in the model. Then all the objects are defined here, such as antennas, phones, phantoms, sources and sensors. Some geometrical objects are predefined such as helical shapes.

It is possible to import CAD files from other programs. SEMCAD can import CAD models in these formats: .SAT .SAB .STL. Use the import model function under the tool menu. It is also possible to export files using the same formats. This means that files from Pro/ENGINEER can be imported into SEMCAD. An example of file importing is in chapter 6.4. In figure 4.1 (next chapter) an example of a model in modelling mode is presented.

Sources can be of three types; edge sources, plane wave excitation sources and wave port excitation sources. The last two types of sources are used for exciting plane waves. Moreover, sensors have to be used to record results from sources. There are different types of sensors that can be used, depending on the type of results wanted. A sensor must correspond to a source type. An edge sensor corresponds to an edge source and should be placed where the edge source is located. The near field sensor is placed at least 2-3 cells outside the objects to display the fields. The volume of the sensor has to be sufficiently large so that the fields can be displayed in the interesting space. The far field sensor should include the model, and the distance to the far field sensor should be at least 5 cells from the radiating structure. The near-to-far-field transformation, which is applied for the computation of the radiation pattern, enables the placement of the far field sensor at a short distance from the radiating structure. The far-field sensor should have a minimum distance of two or three cells from the

boundaries of the computational domain. The near and far field sensors are defined over a volume or an area.

3.2.2 Simulating in SEMCAD

When the model is done the project has to be saved and then moved into simulation mode. The first thing to do is to choose the cell grids. It is possible to have different grid sizes in all three directions, i.e. a non-equidistant grid. Under grid settings/global (see figure 3.3) the extents of the calculation domain is selected, and the boundary type is chosen as either ABC, electric, magnetic or periodic of the outer cells. Finally the stepping is selected in the grid by the minimum step, the maximum step and the ratio. These parameters are defined in model units chosen in the beginning, when opening the project. The minimum step has to be less than the length of any edge sources, since the grid generator cannot reduce them. The maximum step has to be kept low to avoid numerical dispersion. The ratio is how fast the adjacent cells grow. The next dialog box is used for defining the materials and surfaces. They can be defined as PEC, PMC or dielectric (figure 3.4). When using a helical antenna or another complex structure it is important that the cells are connected in order to avoid errors. Otherwise information losses can occur when the grid is generated. This can be avoided by using continuity thresholds. In the third dialog box new grid lines can be defined (figure 3.5), and the rates can be edited between each baseline. There is also a fourth dialog box for sub-grids. This feature of the program cannot yet be used.

Now the voxels (cells) can be computed. It might take a while, especially when using a phantom or a complex model structure with many cells. The program generates baselines at edges of objects that can be edited afterwards. When the voxels have been computed they can be viewed. It is important to check that the different parts of all objects are included in different cells and that all the object parts are connected to each other. Otherwise the computational area has to be recomputed with smaller cells or continuity thresholds on the actual object. The program returns a warning message if an object is not attached to any cell when the computation of voxels is done.

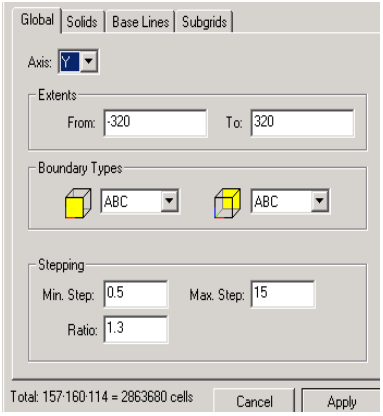

Figure 3.3, The dialog box for grid settings

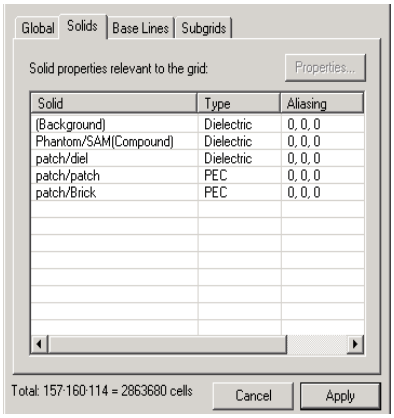

Figure 3.4, The dialog box for materials

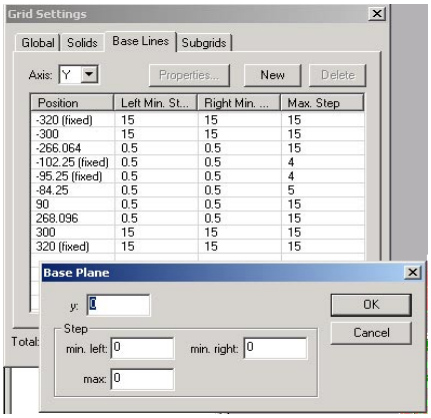

Figure 3.5, The dialog box for grid lines

When the voxels have been calculated; set up for a new run. First choose if the simulation should run in harmonic mode or in transient mode. In harmonic mode the simulation is recording the fields and the simulation signal is a sine. In transient mode the simulation signal is a gaussian pulse signal. The harmonic box has to be checked to make the sine simulation more stable. After this, define the simulation time as

timing unit in terms of periods, time steps or time. Recommended values to start with is, 10 in terms of periods, 10000 in terms of time steps, and 10 ns in terms of time (figure 3.7). These values depend on the calculation domain size, the number of cells and how the other parameters are chosen. When selecting simulation time in time units, TSigma and TPeak has to be regarded if a gaussian pulse is used. The simulation time must at least be 2*TSigma (figure 3.6). The time step from equation 2.16 is calculated automatically in SEMCAD and consequently the CFL condition does not have to be considered here.

The next step is to choose boundary method (figure 3.8). The alternatives are Mur, PML or Higdon (see chapter 2.2.3). Here parameters can be edited, but the predefined are recommended unless the knowledge of FDTD boundary conditions is excellent.

Thereafter, the simulation type has to be chosen as a gaussian sine pulse simulation of many frequencies or a sine simulation with just one frequency. The sensor type must be defined. The edge sensor induces a time varying voltage across the edge sensor gap. It has to be more precisely defined as a hard source, an added source or a voltage source (figure 3.9). A hard source is a source that reflects all the impinging waves. An added source is completely transparent for surrounding fields. A voltage source is a source with internal resistance. This resistance takes out energy of the grid that would otherwise be reflected by a hard source or just be passed through in an added source, but the resistance has no impact on the calculated feed point resistance. If the amplitude is set to zero for a hard sensor, it will act as a short circuit, since the E-field on the edge of the source is forced to the input signal. For an added source with an amplitude value of zero, the source will act as an open loop, because nothing will be added to the fields in the Yee grid. For a voltage source with an amplitude value of zero, the source will behave like a resistor with the specified impedance.

If a sweep in frequency is desired, a gaussian sine is chosen as the simulation signal. Different values has to be defined in its dialog box (figure 3.9). First the centre frequency for the sweep is defined. Then the TShift is set. This says if the signal should start at time different from t=0. Then TSigma, the standard deviation in the time domain, is set. It is the reciprocal value for the standard deviation of the gaussian signal in frequency domain. Next, TPeak should be about 3*TSigma to ensure a smooth start of the pulse. The last parameter is the phase shift, indicating if the pulse is shifted in phase. The simulation time has to be longer than 2*Tsigma, otherwise the simulation will diverge. If TSigma is small the simulated power interval is larger than if TSigma is chosen to be large. These parameters for the gaussian pulse are shown in figure 3.6.

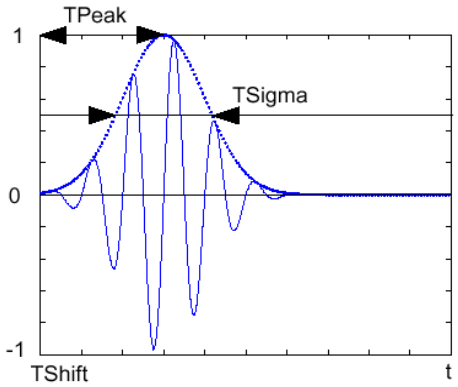

Figure 3.6, The gaussian pulse parameters

In the fourth dialog box a sensor type corresponding to the simulation type has to be defined (figure 3.10). The sensor type must correspond to the source type. A sensor can be used for recording in the time domain or in the frequency domain. For example: running a pulse simulation in transient mode; the edge sensor has to be in the time domain for recording a frequency sweep of Z(f), SWR(f) and |S11(f)|. In this case a field sensor can be used in the time domain. However, this requires a large storage memory in the computer; as the size of the sensor increases rapidly with the size of the computation area. When running a simulation with a sine signal the phasor mode is chosen.

The last dialog box is for defining electric parameters for dielectric materials (figure 3.11). Here, it is possible to predefine electrical constants and then use them again. When all this is done save the project and start the simulation. The simulation time is hard, nearly impossible, to estimate; it depends on the number of cells, the size of the area and the chosen unit for the simulation time. However, the time is usually quite long, ranging from one hour to several days on a standard desktop PC.

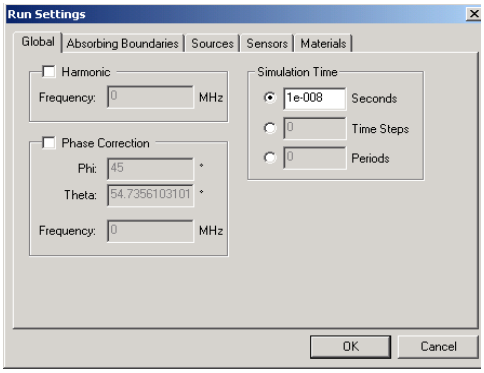

Figure 3.7, Dialog box for time settings

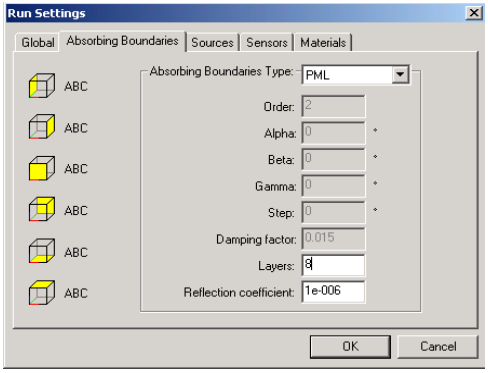

Figure 3.8, Dialog box for boundary conditions

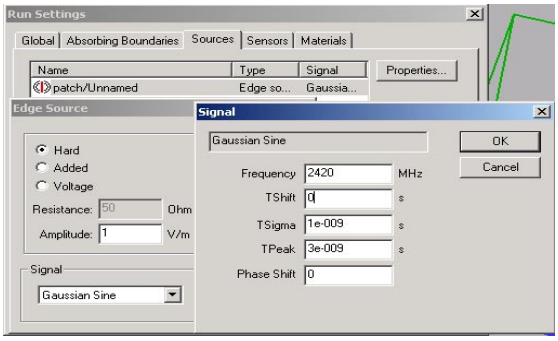

Figure 3.9, Dialog box for first a list of sources, then defining each source and last defining the source signal parameters

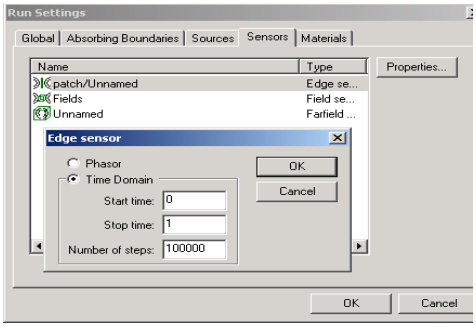

Figure 3.10, Dialog box for sensors

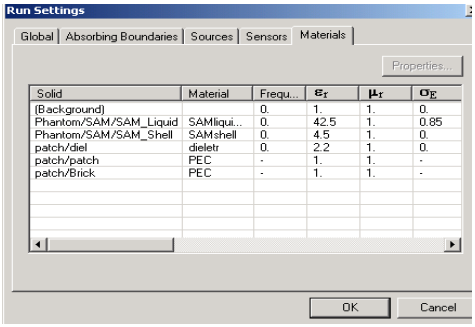

Figure 3.11, Dialog box for materials

3.2.3 Post-processing features of SEMCAD

When a simulation is done the post-processing tree is showed, see figure 4.3 (next chapter). Here the results can be shown from a predefined sensor. A far field sensor or a near field sensor can be used for showing the fields.

The far fields can be expressed in a polar plot or in an XY plot, in logarithmic scale or in mean value scale. Either the two components of the E-field, or the total E-field can be presented. In version 1.2 of the software, an overlay in model can be used. A further explanation of this is in the next chapter. Here the gain, directivity and the total field can be presented. When looking at the far fields the Maximum radiation intensity, the Effective angle, the Maximum values of the E-field and at which angle this occurs, the gain normalised to radiated power, the front to back ratio and the HPBW –Half Power Beam Width, can be found under details.

The power at the feed point is the output power from the edge sensor. From the far field sensor the radiated power can be estimated. A comparison of these two power levels gives a value of the losses in the computational area. When no energy-absorbing objects are included the efficiency should be close to 100 %. When SAM is present the efficiency decreases to 25 %.

The E, H, D, B, S-field and SAR can be presented in three different ways: a contour view, a surface view and an overlay in the model. In all viewers, it is possible to show a cut in the cell layers in three orthogonal directions and show the fields in each layer. All field patterns are in colours and it is possible to zoom into a plot or change the range of plotting, by clicking the right mouse button. When using the contour viewer or the surface viewer, it is possible to show the three different field components in both absolute value and at each instant as the field propagates. In future versions of SEMCAD, it will be possible to show animations of how the field is propagating. The surface view is hard to work with, as the fields are plotted in three dimensions in every slice. The overlay in model is easy to use and the object is included in the picture, but it is not possible to show the different field components. In all three viewers the maximum value can be located under statistics. The plotting method has different features; the field can be plotted with colours, in greyscale, with contour lines and with vectors. The vector method shows the field strength and how the field is oriented.

SAR can be presented in three different ways, in contour view, surface view and in overlay in model. Lots of information can be found under statistical information. Here the mean SAR value, the maximum SAR value and the minimum SAR value are presented, also the total loss in media and the average SAR value. In the readouts under overlay in model it is possible to see the SAR value in every cell, by moving the mouse to the cell of interest.

Post-processing features such as showing the fields and computing SAR takes a lot of time, especially computing the SAR average value over 1 gram. At SEMCAD support, they say that the post-processing computational time is not usually that long and that this is a bug in the software that they will take care of in the next version of the program. In chapter 4 some of the results are shown just to show what different results SEMCAD can generate. This is an easy and useful feature of the program.

All the results can be exported as a plot or as numbers so that they can be used in other software packages. E.g. all calculated fields can be exported to Matlab for further post-processing. The fields are arranged in slices in SEMCAD and when exporting the fields each slice in the program must be exported separately. So if plots in 3D are desired in another program, all field slices has to be exported. Often a hundred slices are used, and that is quite impossible to export. If the output from an

edge sensor is to be used, the file is exported as a .dat file that can be imported in for example Matlab. Matlab uses the commando load for importing a file followed by the name of the file extracted with ".dat.". Be aware of that SEMCAD uses commas as decimal sign while Matlab requires full stops.

3.3 Advantages and disadvantages of SEMCAD

It takes a lot of time to do antenna matching in the program. Yet it is not possible to simulate electrical components as resistors, inductors or capacitors. This will be possible in future versions of SEMCAD. The program cannot optimise the feed point regarding to the object and the input impedance. The source structure is not as complex as in real cases; here it is just a pin. The feed point has to be oriented perpendicular to the co-ordinate system chosen; otherwise connection is lost between the antenna and the phone at the feed point.

Furthermore, the design process takes a lot of time, because when adjusting a parameter the whole simulation has to be recomputed. If the purpose of the antenna design process is to try a new antenna structure and perhaps optimise it, SEMCAD is not the best tool today. The program is not for use in the first step of the antenna design process, software packages such as IE3D are more suitable.

The version of the program used for this thesis is at first version 1.0 and then version 1.2. In November 2001 the version 1.4 is supposed to be released, probably with more and better features. Version 1.2 has some bugs. The SAR calculation takes a lot of time in the post-processing stage, and sometimes it cannot compute SAR at all. Another important feature that will be implemented in future version of SEMCAD is the sub-grids; grids that can be chosen to be smaller in an interesting area. This is necessary for complex structures; otherwise the number of cells will be too large. This will also reduce the computational time.

Here follows some piece of advice that can be useful when simulating in SEMCAD:

- For helical antennas, the continuity thresholds have to be checked and used. The continuity threshold couples the adjacent cells to each other, so the helical antenna is just one body. If not, connection can be lost on a segment of the antenna and the results are useless.
- Sometimes a diverging simulation occurs, however this is most often when time steps are used as simulation time. It is better to set the simulation time in seconds. Then the program computes the sufficient time for the simulation. This is only when using a pulse simulation, when using a sine simulation the period time is better to use as time measurement.
- The output power seems to be small and the antenna does not seem to radiate any power. In the simulation set up, it is not possible to set the input power to the system. The input source voltage can be set to a value when using a voltage source, otherwise for other sources the input voltage is 1 V. There is no use computing with another value, since the calculations are linear. So when calculating the fields the power has to be normalised to 1 W. When using a hard source the input voltage is approximately 10^{-6} V and the input current is approximately 10^{-6} A too. This gives the approximated power (P=I*V) 10^{-12} W. What should be compared is the input power and radiating power. This number shows the losses in space.
- When measuring SAR for 900 MHz the standard power transmitted is 250 mW. When calculating SAR the power has to be normalized to 250 mW and

not to 1 W. If not normalized to 250 mW the computed SAR value should be divided by 4. For 1800 MHz the standard power is 125 mW.

- When simulating with PML boundary conditions the program splits the outer cell on the boundary edges to avoid radiation back in the cells again. Then the simulation will take longer time than when using Mur. PML is mostly used when the simulation area is small.
- When putting a cellular phone near the head, the head acts like a large dielectric load. The antenna parameters changes and the antenna has to be redesigned with another shape. This is a disadvantage of the program. It probably depends on the lattice structure around the device, and when using a phantom the lattice is maybe too large for computation.
- When SAR computations are done and plastic materials are included in the model, the dielectric voxles cannot be checked when computing the SAR value. If checked, the SAR value is also computed in the plastic material and that is not the wanted SAR value.
- Always check the voxels before starting a simulation so that the cell pattern of the object is similar to the real object.

For more information about SEMCAD, please see the reference manual [7] or contact SPEAG. In chapter 4, figures and results of a SEMCAD simulation is shown for a helical antenna.

4 Simulation of a helical antenna

To investigate the performance of the program; a helical antenna on a metal box is simulated. The helical antenna has a fairly complex structure so this is a good test of how the program behaves. The point of the simulations in this chapter is to see how the matching procedure can be done in SEMCAD and what the programs output results are.

The metal box used was 130 mm long, 49 mm wide and 23 mm deep. This is the dimension of a real phone on the market that will be used in chapter 5 and 6 when measuring and simulating real cases. A quarter-wave helical antenna for 900 MHz is tested with different physical dimensions just to obtain the matching at 50 Ω. The antenna was also moved on the top of the box to see if the antenna parameters changed. The helical antenna is used in normal mode.

It was quite difficult to find the right matching. Just to know where to start a first sample came from [8]. Prior to these simulated results, all the dimensions of the antenna was varied, as the diameter of the antenna, the length of the antenna, the diameter of the wire and the pitch angle to see how the resonance frequency changes. The final antenna dimensions had a length of 32 mm, a pitch distance of 9.5 mm, a diameter of 10 mm and a wire diameter of 1 mm. The final phone with antenna is shown in modelling mode in figure 4.1.

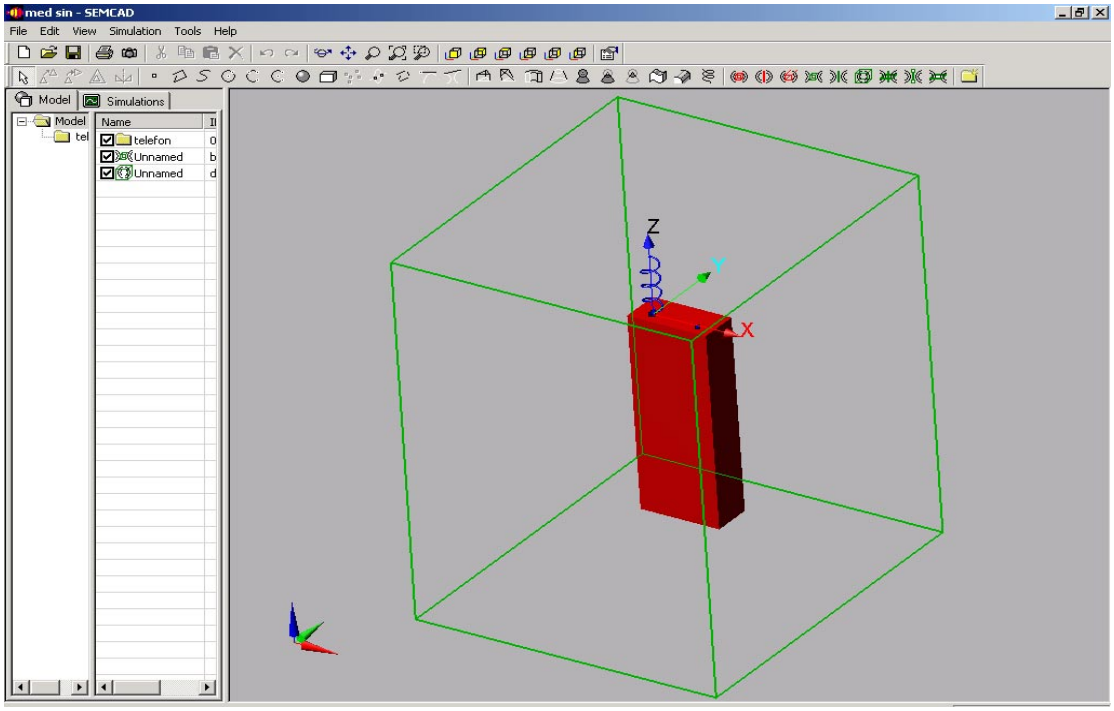

Figure 4.1, A helical antenna in modelling mode, with a far field and a near field sensor

The project is saved and moved to simulation mode where the cells are generated. For this project the minimum step is 0.5, the maximum step is 3 and the ratio is 1.3 for the X and Y-axis and 1.05 for the Z-axis, explained in chapter 3.2. In figure 4.2 the voxels are shown and in this mode it is possible to see if the entire object is attached to voxels. The surfaces are all PEC, and the continuity thresholds are used for the antenna. Here the non-equidistant grid is used, concentrated on the antenna in all three-dimensions.

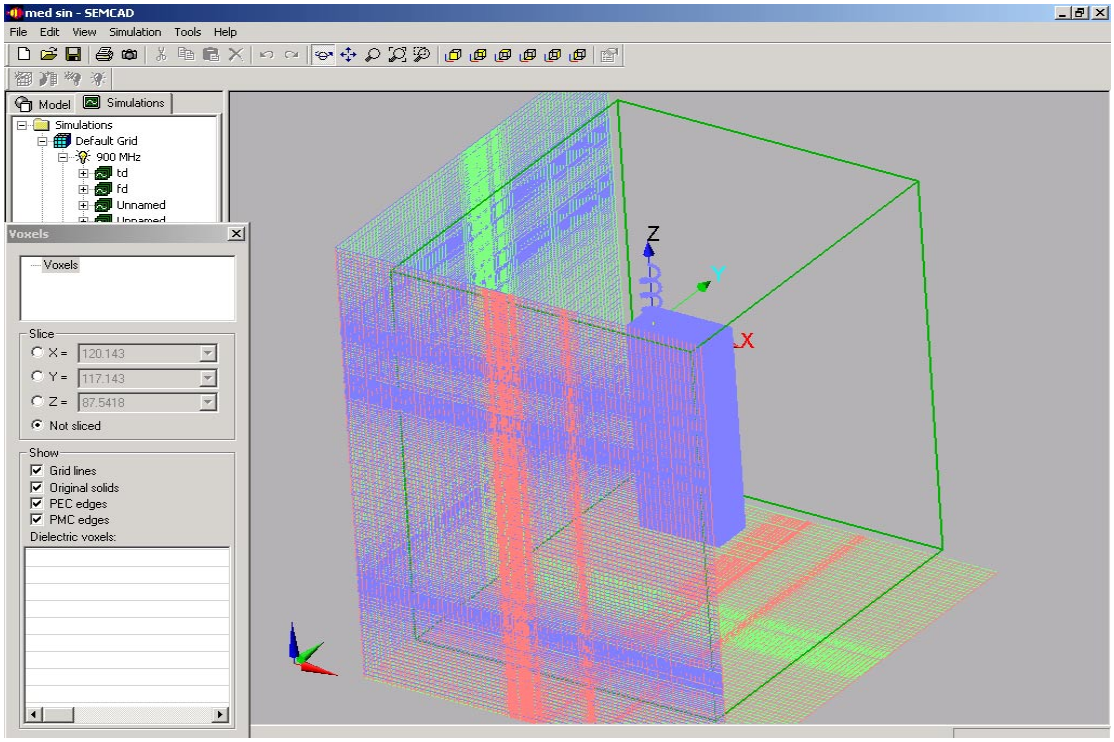

Figure 4.2, The helical antenna with 2 million voxels

After generating an acceptable grid a new simulation can be run. For this simulation a sine simulation is run with PML for 900 MHz. In order to save time a voltage source is used and the simulation time is 10 periods. The simulation takes nearly two hours. In figure 4.3 the post-processing tree is shown with all the results for the helical antenna in harmonic mode.

The first sensor is a time domain sensor that shows the voltage and the current at the edge sensor. When using a sine signal, the voltage plot and the current plot should be periodic signals; if not, the simulation has diverged. This sensor is more interesting when using a pulse signal. The second sensor is in the frequency domain and this sensor gives values of the voltage, the current, the impedance, the SWR, the S11 and the power at the feed point for the specified frequency, here at 900 MHz. The third sensor is a near field sensor, presenting the near fields. The fourth sensor is a far field sensor showing the far fields and the radiated power. In chapter 3 the different options for displaying are explained more in detail.

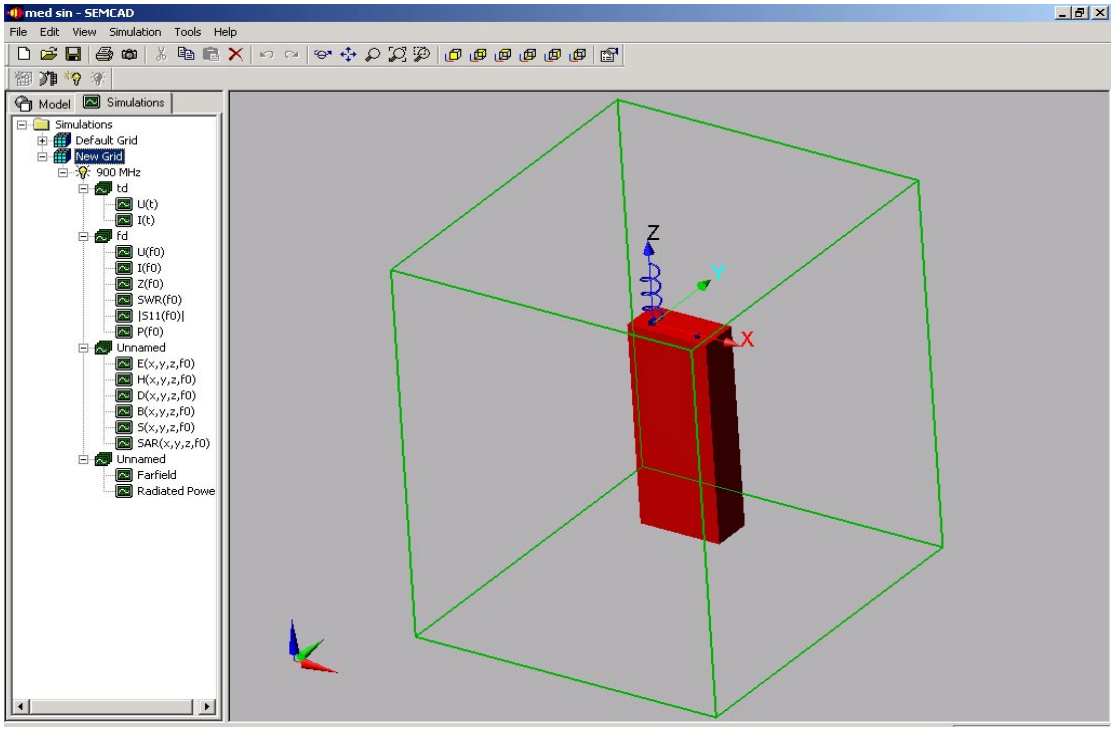

Figure 4.3, A helical antenna with the post-processing tree.

Another simulation using a pulse signal, with the same project and the same grid, is done to see at which frequency the resonance is located. In this case an edge sensor in time domain recording simulated results is necessary. The first two results are the voltage and the current. Always check these plots to see if the simulation is diverging. The results are then presented as in the following figures as a function of frequency. Figure 4.4 shows the Smith Chart of the impedance for the simulation. It is possible to see the impedance as an ordinary XY plot, showed in figure 4.5. The dashed line is the imaginary part of the impedance and the solid line is the real part of the impedance. The imaginary part changes signs at approximately 900 MHz.

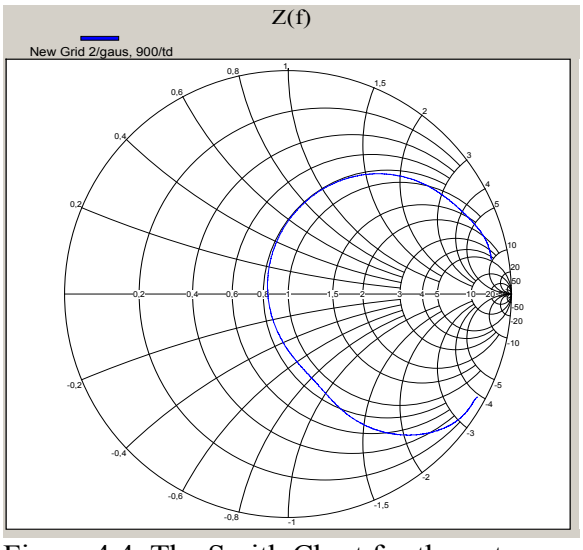

Figure 4.4, The Smith Chart for the antenna

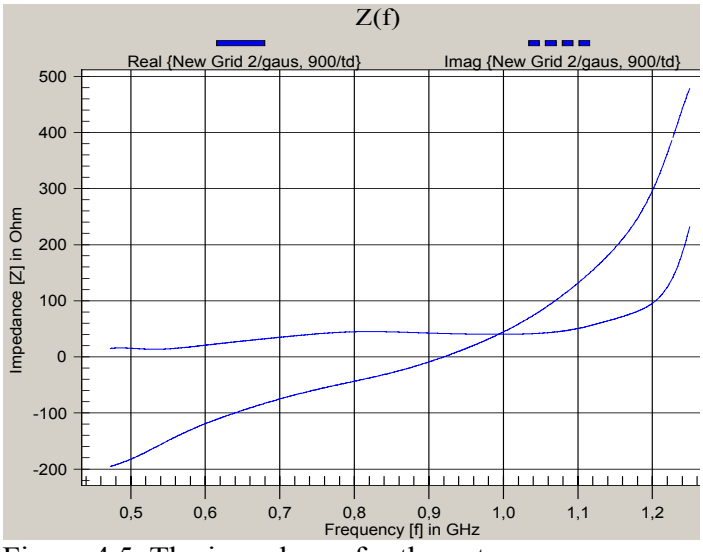

Figure 4.5, The impedance for the antenna

Figure 4.6 shows the standing wave ratio of the antenna. The bandwidth, defined as when SWR is less than 2, is 830 MHz to 980 MHz, i.e. 150 MHz. Figure 4.7 shows the S11 or the return loss. To define the same bandwidth as for the standing wave

ratio the S11 has to be less than –10dB. In this figure the resonance frequency is at 920 MHz. Furthermore the input power can be shown, however, in this case it is not so interesting to show. The power plot shows at which frequencies the energy is transmitted to the antenna.

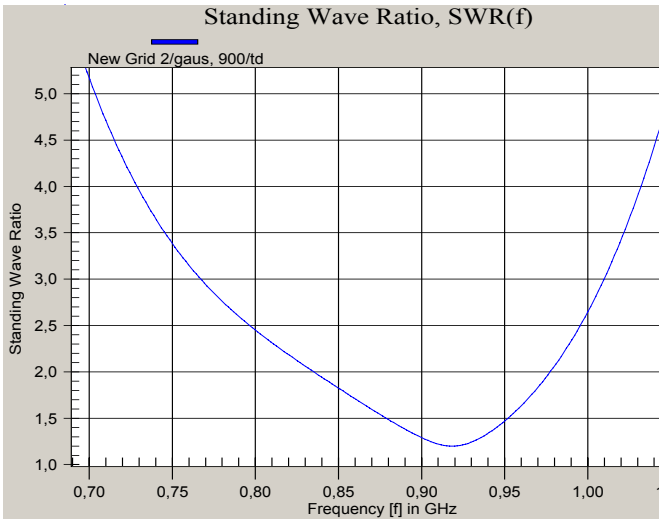

Figure 4.6, SWR for the helical antenna

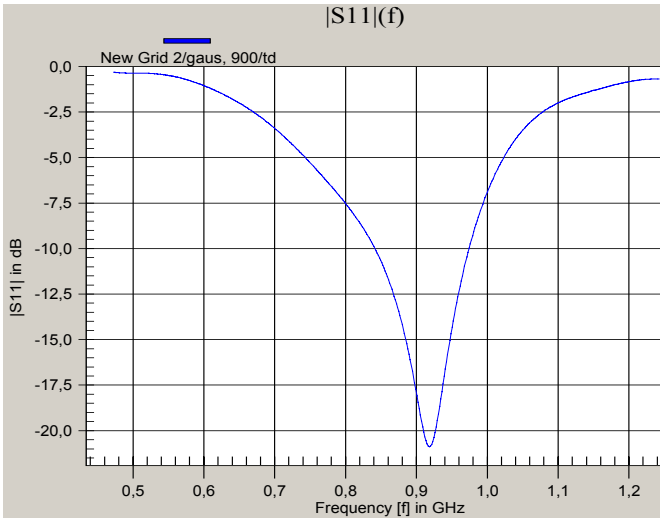

Figure 4.7, S11 for the helical antenna

In the sine simulation the E and H-fields are presented. In the following figures the fields are plotted with contour curves. The area is cut in the Y-axis, where Y=0, and the XZ plane is exposed. The figure 4.8 is the total absolute value of the E-field at a cut on the surface on the phone. This figure shows that the field lines are concentrated at the antenna, at the top of the phone and at the bottom of the phone; there are also large currents on the sides of the box. The metal box has nearly a length of a half-wavelength for 900 MHz. The figure 4.9 is a cut through the antenna; here the field lines are concentrated on the radiating helical structure. The metal box is assumed to be a perfect conductor and as a result, there are no fields inside the box.

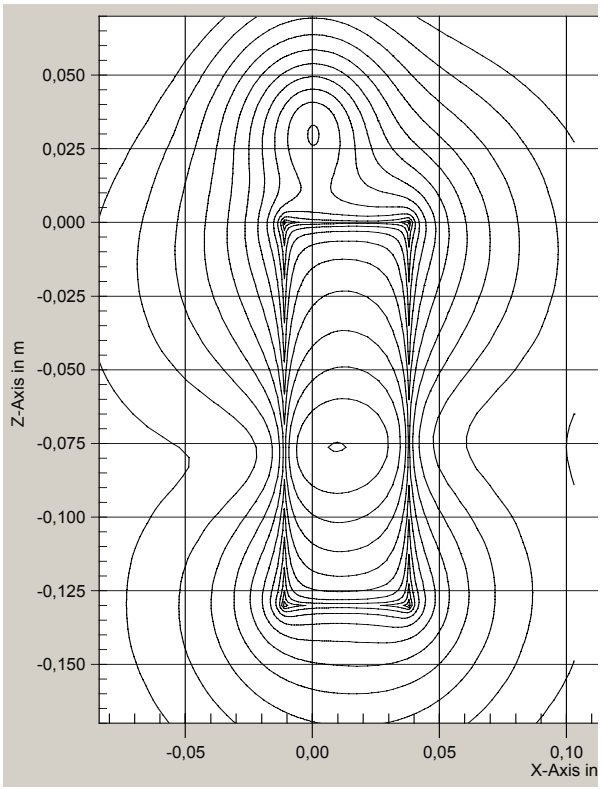

Figure 4.8, E-field on the surface of the phone

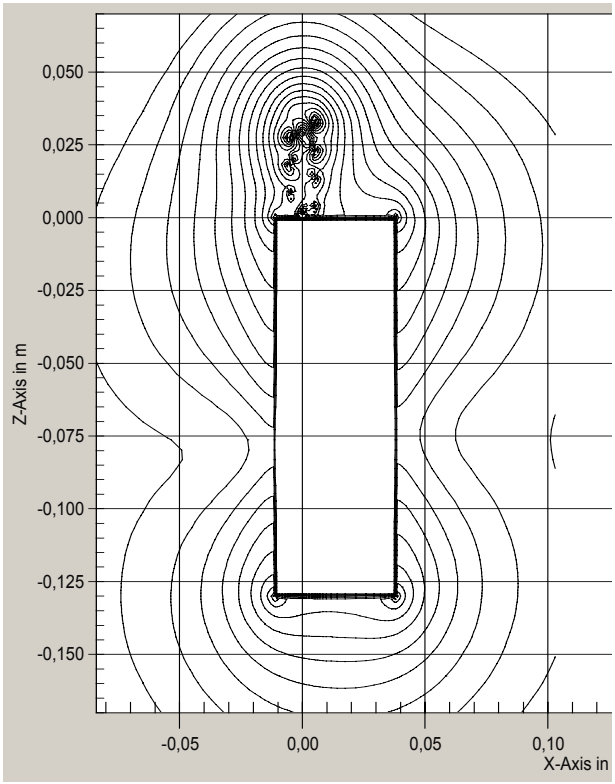

Figure 4.9, E-field cut through the antenna.

In SEMCAD, each component of the fields can be shown. Here the E-field components are shown. Figure 4.10 is the E_x-component, figure 4.11 the E_y-component and figure 4.12 the E_z-component. In figure 4.13 the H-field is shown in the same cut.

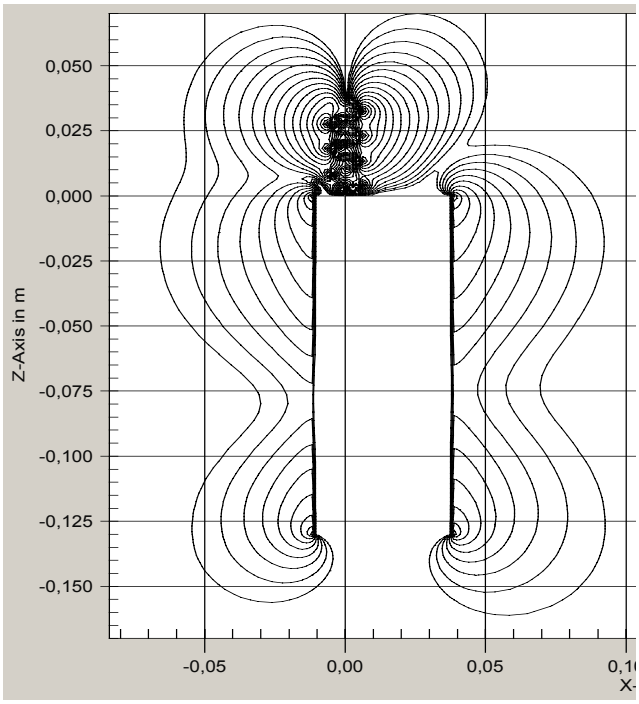

Figure 4.10, The E_x-component

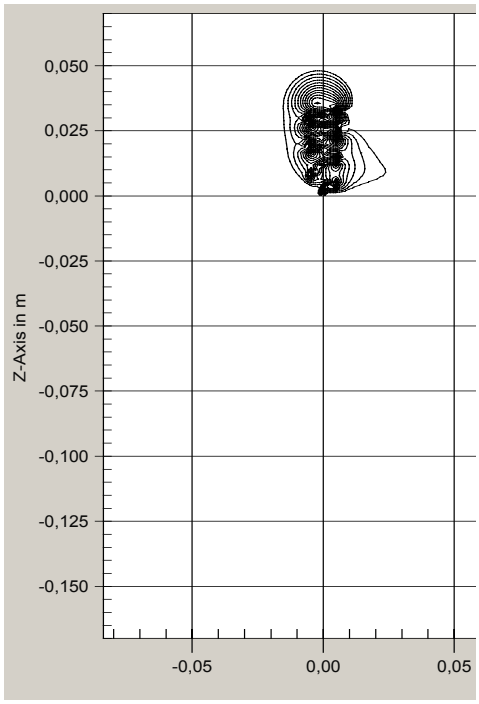

Figure 4.11, The E_y-component

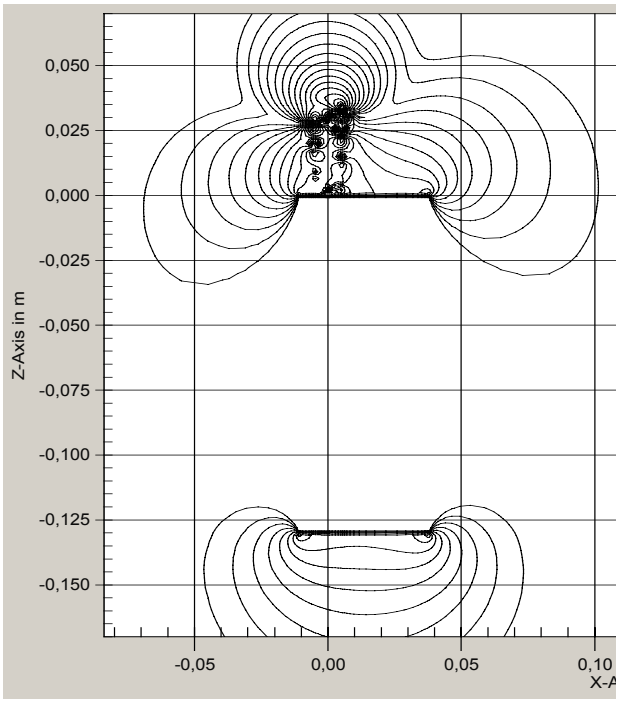

Figure 4.12, The E_z-component

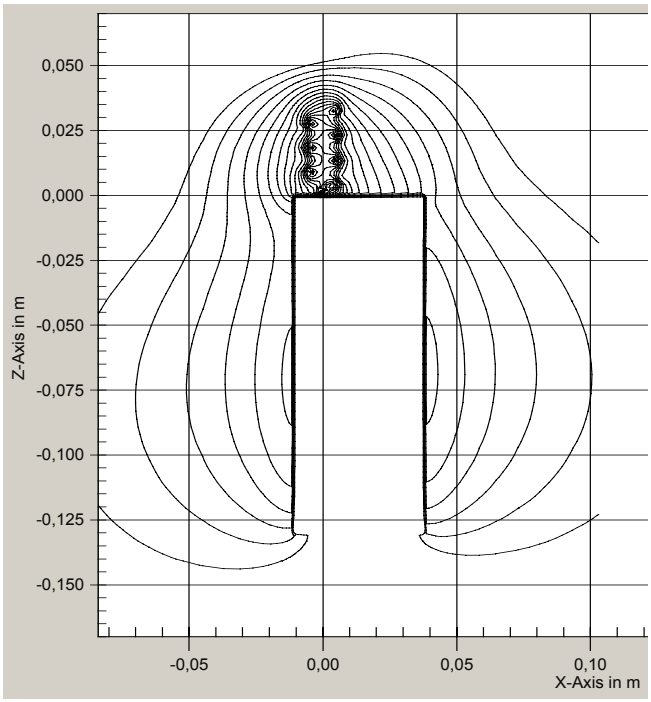

Figure 4.13, The total H-field

In figure 4.10 it is easy to see that the charges are distributed along the phone surface. The field is concentrated on the radiating antenna. In figure 4.11, the field is nearly zero because the cut is in the Y-direction and the field component is also in the Y-direction. At this point, the fields are always close to zero. In figure 4.12, the charges are more concentrated on the helical structure because the width of the wire is smaller than the width of the metallic phone box. The H-field in figure 4.13 is the complement to the E-field in figure 4.9. Here, where the E-field has a maximum the H-field has a minimum and where the H-field has a maximum, as on the centre along the metal box, the E-field has a minimum.

Now, the phone can be used together with SAM to calculate the SAR value. This is done in chapter 6.1 when simulating real cases with a helical antenna placed on the right hand side on the top of the phone.

In reality, the antenna is covered with a plastic material to protect the antenna from its surroundings. This plastic material induces losses to the transmitting and receiving electric field. Here simulation is done to compare the resonance frequency in these two cases, with or without a plastic cover. The plastic cover used in this simulation has the following dimensions and parameters; $\varepsilon_r = 3$ and $\sigma = 0.0003$ A/Vm and the thickness is 2 mm, placed outside the antenna. The projects are run with the same grid size and the same simulation time. See figure 4.14 for the results. As seen in the plot the resonance frequency decreases when the plastic cover is present. The antenna must now be redesigned to compensate for the plastic cover. The decrement is large; this might be because the conductivity for the plastic was chosen too large in this case.

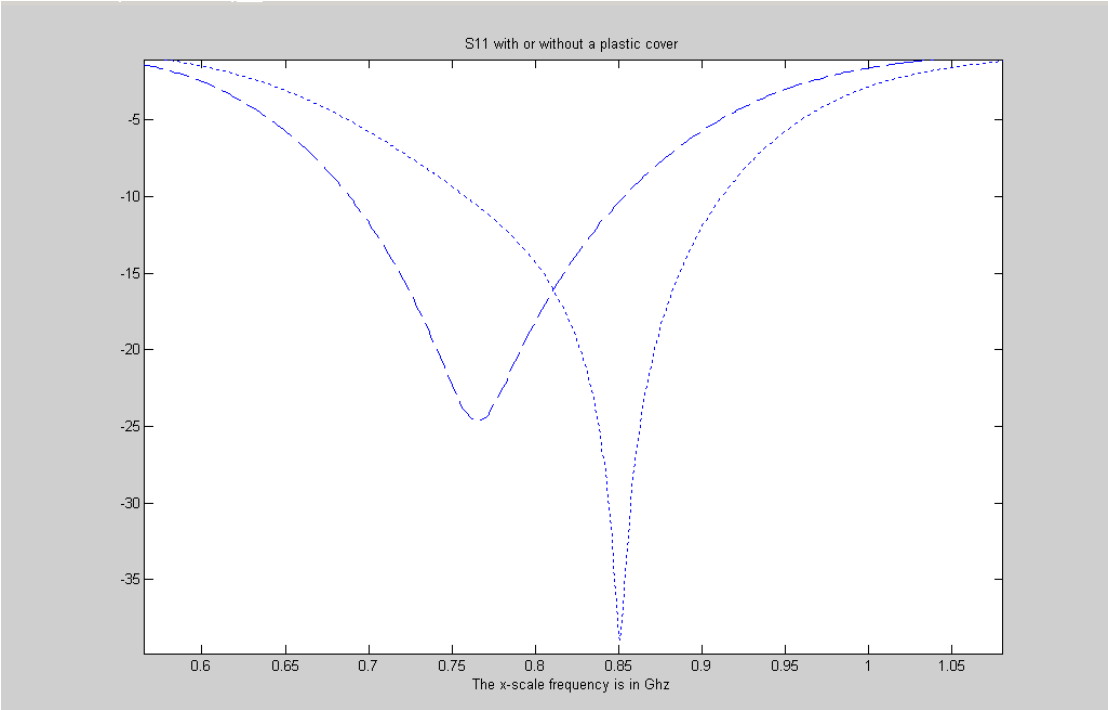

Figure 4,14, The helical antenna simulated with or without a plastic cover. The dotted line is without a plastic cover and the dashed line is with a plastic cover. The same grids are used in both cases.

The difficulty of simulating a helical antenna is that the simulated results depend a lot on the grid size. For example the SWR plot had large variations, see figure 4.15. This depends on how the grid generation is done over the complex helical structure. The helical antenna is a circle in the XY plane and then spread over a large volume compared to the straight quarter-wave whip antenna in the same plane, and the wire is so thin that when the area is divided into cells, the cells are coupled differently in each case of cell grids. The grid generation is not done compared to the object; the space is just divided compared to the ordinary XYZ components. This means that the grid does not follow the structure; if more than 50 % of the cell is occupied by an object, the entire cell is set to be of that object, otherwise the entire cell is set to the surrounding media. This can definitely change structures, and when working with large grids this gives incorrect results because the simulated object is not a copy of the real object. For a more simple structure such as a wire the SWR does not change much when the grid is changed.

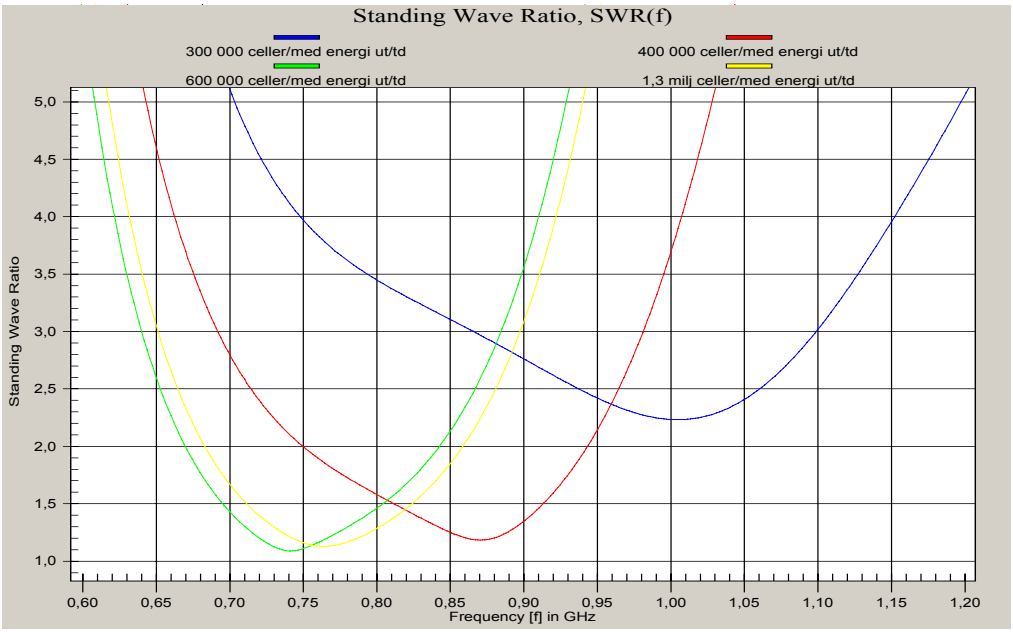

Figure 4.15, SWR plot with changing grid size. All other input parameters are constant. The plotting scale is from 0.6 to 1.2 GHz in X and 1.0 to 5.0 in Y. The first curve is with 600 000 cells, the second with 1.3 million cells, the third with 400 000 cells and the last with 300 000 cells.

More simulations were done to find an optimum for cell sizes compared to the resonance frequency. Another question is if the resonance frequency depends on the minimum step, maximum step, the ratio or just the number of cells in a predefined area. The results are presented in a Matlab plot, see figure 4.16. In this plot the resonance frequency varies over a large range of frequencies for small number of cell grids. The amount of simulations is too small to say if there is a dependence between the resonance frequency and the minimum step, maximum step or the ratio, but clearly there is a dependence between the resonance frequency and the number of cells. A good rule of thumb is to minimise the maximum step over the object.

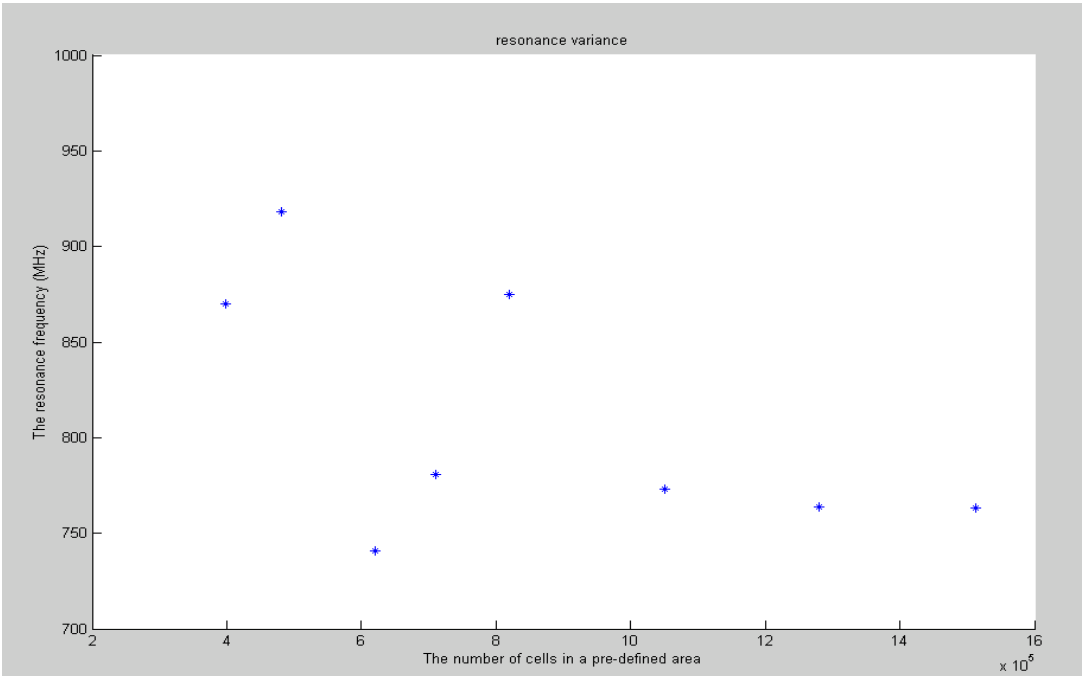

Figure 4.16, The resonance frequency depending on the number of cells

The diverse result depends on the complex structure of the helical shape. When the number of cells is too small or if the maximum step is too large, the shape in the computed voxels is not a helical structure anymore, just a fragment of cells that is not connected to the adjacent cells. The minimum step must be small enough and the maximum step cannot be too large. When using these kind of complex objects the baselines must be edited to have a more concentrated computational area over the interesting structure. An illustration of the importance of the cell sizes is shown in the following figures, both showing the same helical antenna from the same view. In figure 4.17 the grid is too coarse, to improve this example, the maximum step can be reduced. In figure 4.18 an acceptable grid structure is shown.

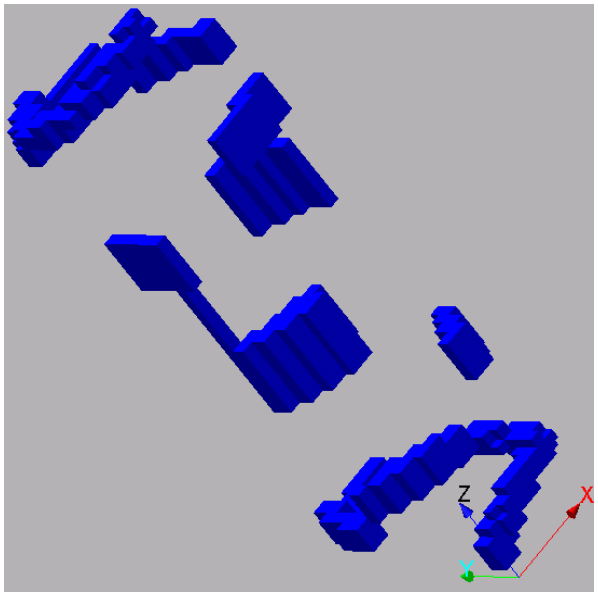

Figure 4.17, A helical antenna with unacceptable grids; min. step 0.5, max. step 5 and ratio 1.3

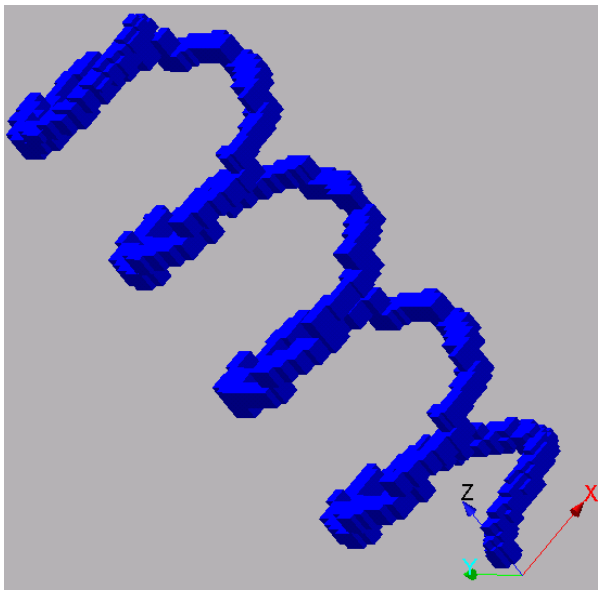

Figure 4.18, A helical antenna with acceptable grids; min. step 0.25, max. step 1 and ratio 1.3

Now when knowing how the simulations depend on the number of cells; the time dependence of the results had also to be examined to tell when stability is reached. In figure 4.19 three simulations are done, however only two curves are observable. The first curve has a simulation time unit of 5 ns and the other two curves, which cannot be separated in this figure, one has a simulation time unit of 10 ns and the other has 20 ns. The simulation time unit 50 ns is used too, but not in the figure; the result was the same as for the simulation of 10 ns and 20 ns. The simulation with longer simulation time is more stable for a larger band and the results are more confident. Here it can be helpful to look at the voltage plot since this result shows the input voltage and if it has reached stability or not. If this curve is still oscillating the simulation has to be redone with a longer simulation time unit.

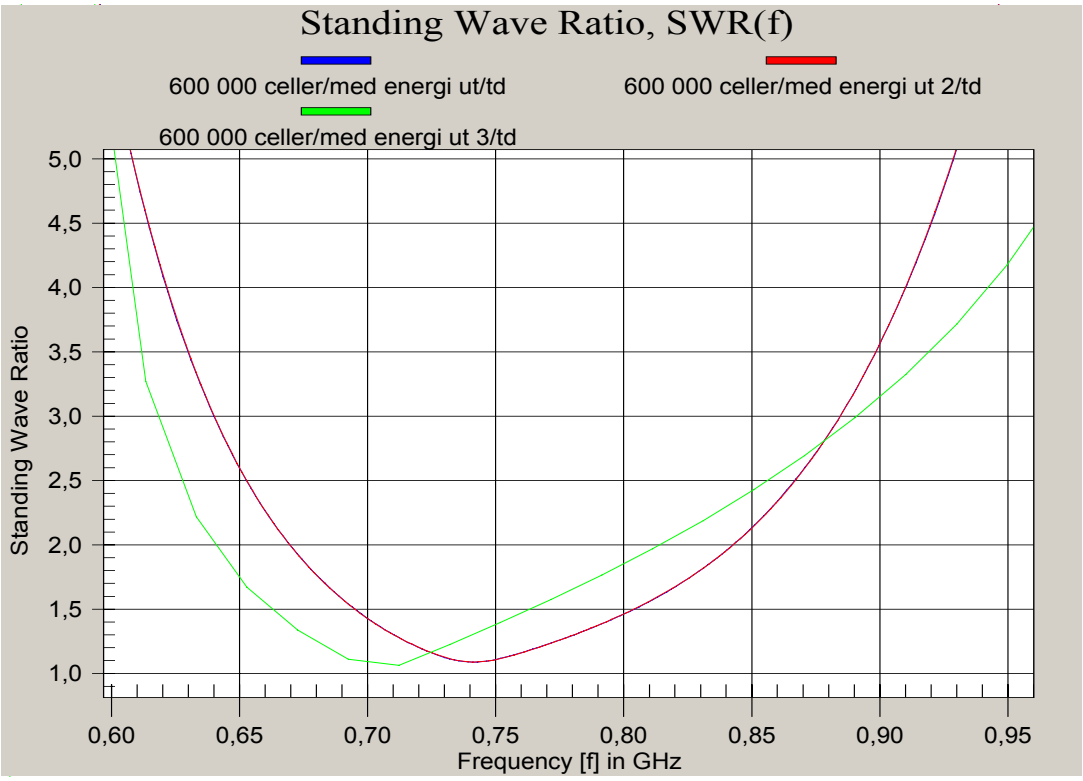

Figure 4.19, The standing wave ratio for simulations with different time units. The first curve is the 5 ns and the second is the 10 ns and the 20 ns.

The conclusions are that the cell size has to be kept sufficiently small, the number of cells sufficiently large and the simulation time sufficiently long. It is not easy to say how small the grids should be, or how long simulation time or how many cells that are needed. This depends on the complexity of the simulation object. Here, the object is three-dimensional and consequently the maximum step has to be kept small within the object. Without sub-grids, as in these examples, the simulation time is large, but with sub-grids the simulation time will be acceptable. The time simulations are stable here after 10 ns in time unit. This is true for this simulation and many others; however, check the voltage and the current in a time domain sensor to assure that the simulation time is long enough.

It is difficult to have a clue about how long a simulation takes. It depends on the number of simulations run at the same time on the computer, if the computer is used for other things as writing and of course of the simulation set-up. SEMCAD always estimates the simulation time and how much time that is left for the simulations. The helical antenna was run in transient mode with 1.1 million cells for 5 hours and with 500 000 cells for 2 hours. In harmonic mode the simulation was done with a sine signal for 6 hours with 2 million cells.

5 A parametrical study of the touch position

When doing measurements and simulations in the talk position, the phone is placed near the ear. The phone should be placed and turned according to the measuring standard used. This position should be what is called the touch position, the position where the phone touches both ear and cheek. For the CENELEC standard the phone should be placed as shown in figure 5.1. First the phone is placed in the line between the ear and the mouth. Then two cases should be examined: one when the lower part of the phone is turned 10° away from the face in what is called the 100° position. The other case is when the lower part of the phone is turned 10° towards the face into what is called the touch position.

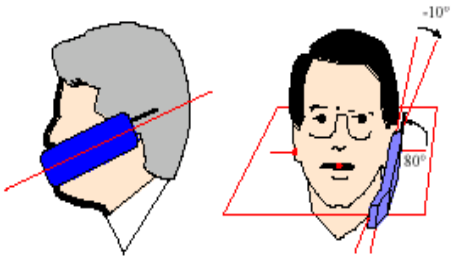

Figure 5.1, How the phone is placed and turned near the head to find the touch position, from [9]

An interesting question is where to place the phone. Is there a theoretically optimal position where to place the phone, and if yes: where is this point located? A reference point on the ear is predefined on SAM, but the corresponding position on the cellular phone utilised is not predefined. The position has to be estimated based on where the loudspeaker is placed on the device. If a file is imported from a CAD program, the loudspeaker is already in the model.

What influence does the position of the phone have on the SAR value? Does SAR differ a lot when the phone is moved 1 or 2 mm from the initial position? A well known fact is that when the phone is moved just one mm outwards from the head, the SAR value decreases with nearly 25 %; however this is not relevant when the phone is moved parallel to the head. In this chapter, simulations and measurements are compared to each other. Chapter 5.1 will deal with measurements and chapter 5.2 is about simulations. The last chapter is a comparison between the two phantoms.

5.1 Measurements of the touch position

The measurements are done at Moteco in Lund on the DASY3 system, see figure 5.2. The system is designed by SPEAG, the same company that has made the software. The robot is controlled by a computer and while measuring, the probe moves back and forth in the liquid to find the maximum value of the E-field. Then the SAR value is calculated by the computer. SPEAG's homepage has more information about DASY3. An article about how measurements with DASY3 are done is recommended for the interested reader [10]. The cellular phone is placed under the phantom in the touch position. Then, if it is connected to a local base station, to which it makes a call, the base station will control power levels and the channel.

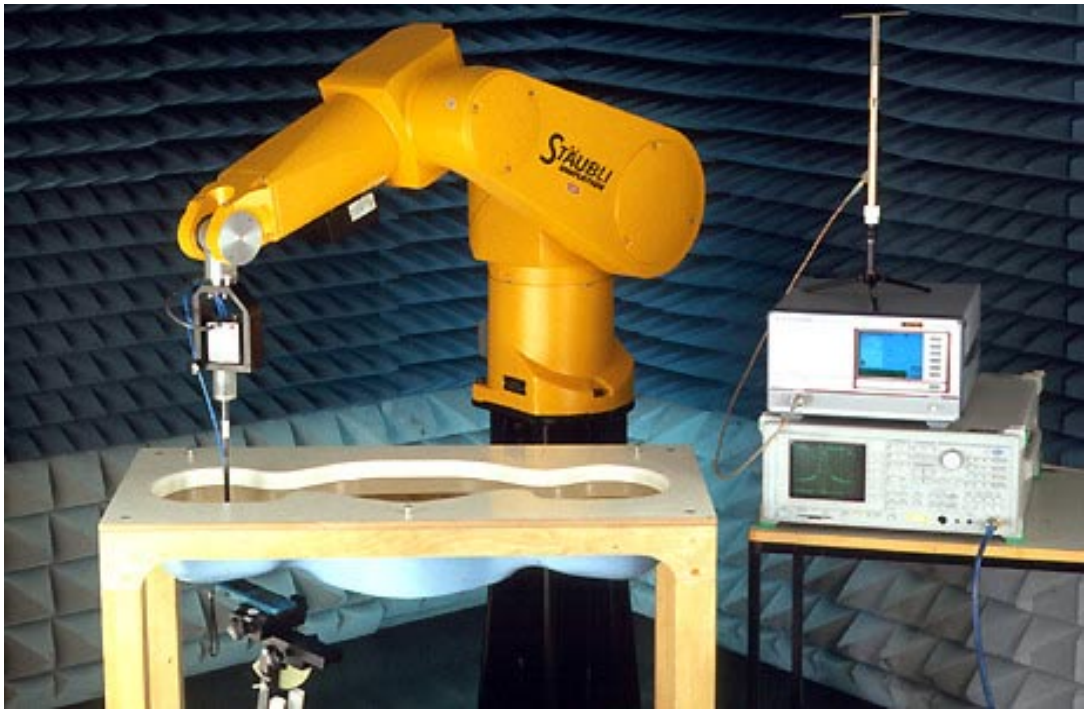

Figure 5.2, The measurement arrangements with DASY3 from SPEAG's homepage

The phantom used in these measurements is the generic twin. This is the same phantom that can be used for simulations, see chapter 3.1. In the phantom the biological tissue is represented of two materials, first a 2 mm plastic shell and then a liquid made of a mix between water, sugar and salt. The mix is made with different proportions for different frequencies so the liquid corresponds to the electrical parameters for brain tissue at a specific frequency.

The touch position is hard to find for the generic twin phantom. To compare measured results the phone has to be placed exactly in the same way in every single experiment, otherwise measuring errors as large as 10 % can occur.

The measurements are done on a standard cellular phone. The telephone is rather simple, just a box and a single band helical antenna; it has the same dimensions as the simulated phone in chapter 4. All measurements are done with a local base station for the GSM band, between 880 and 960 MHz. Here, only one cellular phone is examined but the results are expected to be similar for other phones. Maybe the results from a cellular phone with internal antennas would differ. If the results differ, this depends on the currents on the chassis.

The first measurement was done with the loudspeaker placed right under the ear of the phantom. The phone was turned into the touch position. After that the phone was moved in the range -30 mm and +30 mm in the direction up/back and down/forward. This direction is parallel to the line in figure 5.1. The phone was still placed in touch position. The phone was placed on the right hand side of the head. These series of measurements were done at different times and the phone was moved from its position between each attempt. This is an error source for the measurements.

The standard for measuring SAR says that the phone should be transmitting with full power. However, full power was not used during these measurements, due to the fairly low battery capacity. Since full power is not used the SAR values can only be compared relatively to other measured results with full power. Several series of measurements have been done on the same device in order to provide confident results. The results are plotted in figure 5.3.

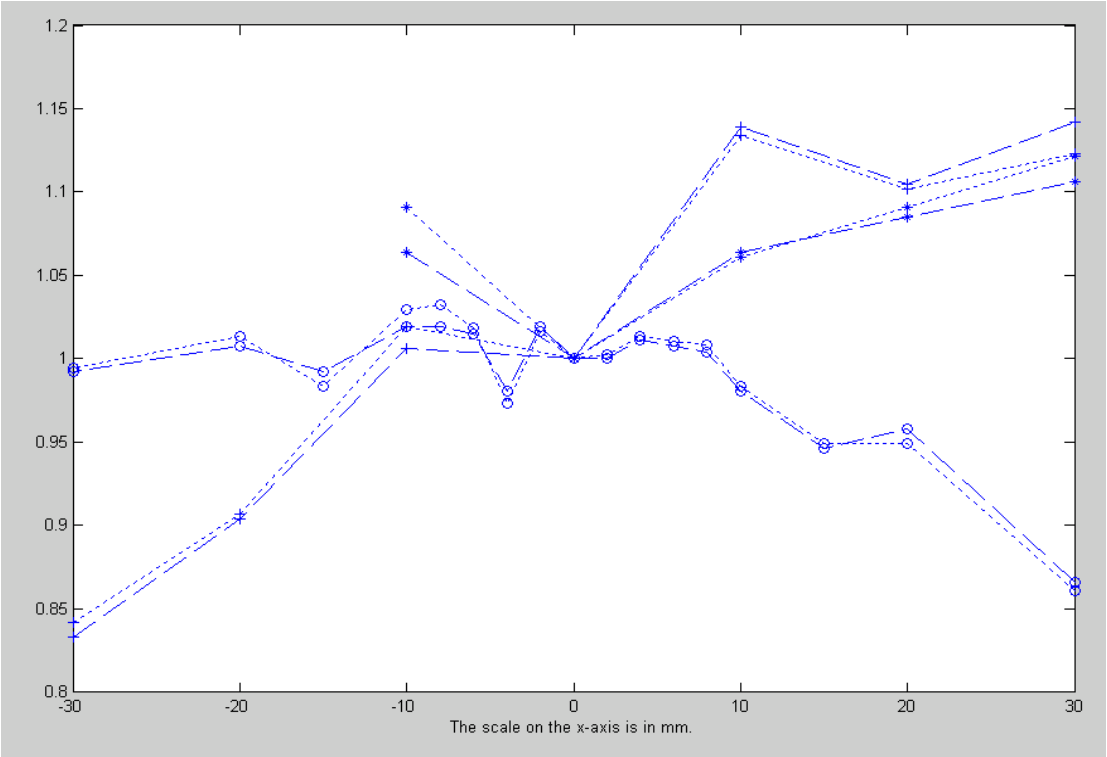

Figure 5.3, The SAR variations when the phone is moved back and forth. The dashed line is the SAR averaged over 10 grams and the dotted line is SAR averaged over 1 gram. The points marked with "*" are from the first measurement series, the points marked with "+" are from the second series and the points marked with "o" are from the last measurement series. All values are normalised to the value at the "mid-point".

From these measurements it is clear that the position of the phone along this axis does not have a great impact on the SAR value. The variation of SAR for 5-10 mm deviations is less than 10 %, but for certainty, more measurements have to be done with different cellular phones. An error source in the first two measurements is that they were not done in the same number of attempts as the third series. It took me a while to learn how to place the phone in touch position, so for that reason the last series is more reliable than the first ones.

One measurement sequence was done where the phone was moved forward (relative to the head) and backward, see figure 5.4. Only five measurements were completed. Due to the few measurements, the results are not reliable.

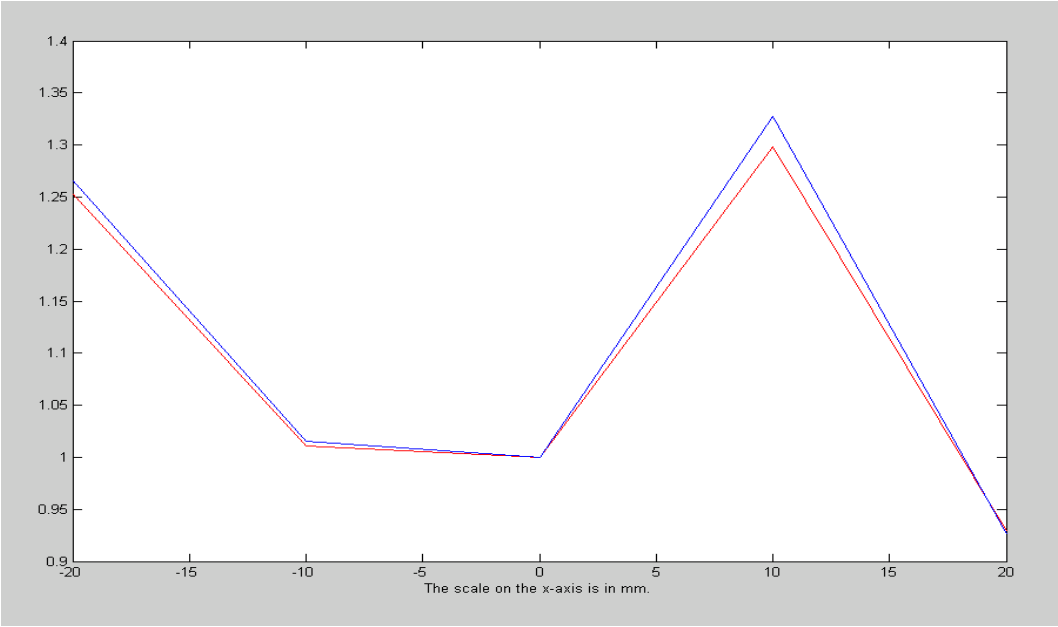

Figure 5.4, The SAR variations when the phone is moved forward and backward relative to the head.

The conclusion from all these measurements is that if the phone is moved 2-3 mm from the original defined position, the SAR variation is less than 10 %. This is in the same size as normal measurement variations. The SAR value does not differ very much for these measurements and therefore no further investigations are done.

5.2 Simulations of the touch position

The phone model in chapter 4 is used here, but with SAM instead of the generic twin phantom. A discussion of why this phantom is used, and what the differences are between the models are done in chapter 5.3. See figure 5.5 for SAM and the phone with the computed voxels. It is quite hard to find the touch position in SEMCAD, but there is a tool for cutting the model and displaying where the phone touches the phantom. This tool is found in simulation mode under view/clipping.

Unfortunately the edge source has to be placed perpendicular to two of the axes, otherwise problems will occur with the feed point and the source will not couple together the two simulated objects. As a result, when simulating with a phantom, the phantom has to be rotated and not the phone. In SEMCAD the rotation feature is hard to use. The object is rotated an angle around an axis that the user defines. Here the clip tool can be useful to see where the object touches the phantom.

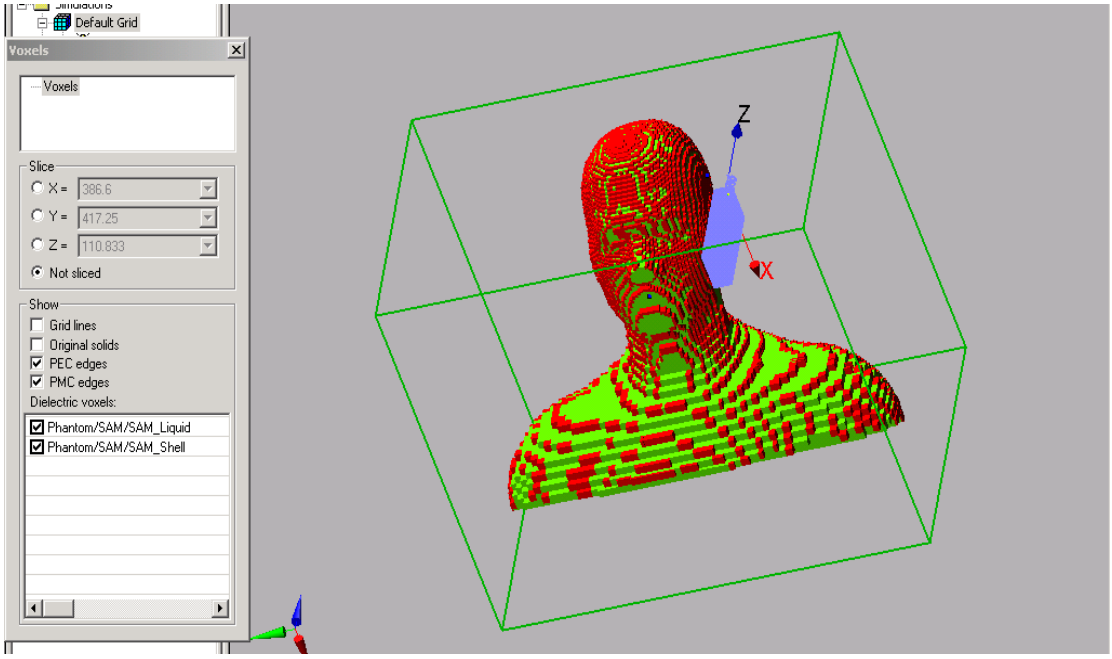

Figure 5.5, SAM with computed voxels. The phone and the antenna have PEC conditions and the SAM model is dielectric.

A problem occurred with this phone. When placed near the model head the phone was no longer within the 2:1 bandwidth (SWR<2.0). This is because SAM is a large dielectric load and the antenna cell generation cannot be made sufficient small on a computational area as large as this one; the simulation time will increase to several weeks if the area is chosen as large as wanted. To decrease the impact from SAM on the antenna parameters, the phone was moved one mm away from the head and then again the antenna was within the bandwidth when simulating. To avoid the large impact of SAM and to simulate a case more close to reality, a plastic cover was placed over the antenna to obtain a more stable outcome, see chapter 4, figure 4.14. However the phone was still not within the 2:1 bandwidth.

These complex problems were also simulated with a quarter-wave antenna, called a whip antenna. The phone was placed first in the original position and then moved back and forth along the same direction as in the first measurement series. Here another problem occurred: it was impossible to calculate the SAR value averaged over 1 gram, because of a software bug. See the results from these simulations in figure 5.6.

A simulation was done for this quarter-wave stub antenna for a frequency not within the 2:1 bandwidth. The SWR value was 2.2 and the SAR value was 1.44 W/kg. For the antenna within the bandwidth, the SWR value was 1.05 and the SAR value was 1.51 W/kg. This is a large difference for the antenna just outside the bandwidth; the SAR value would be much lower if the antenna had a larger SWR. So you should always keep the antenna within the actual bandwidth.

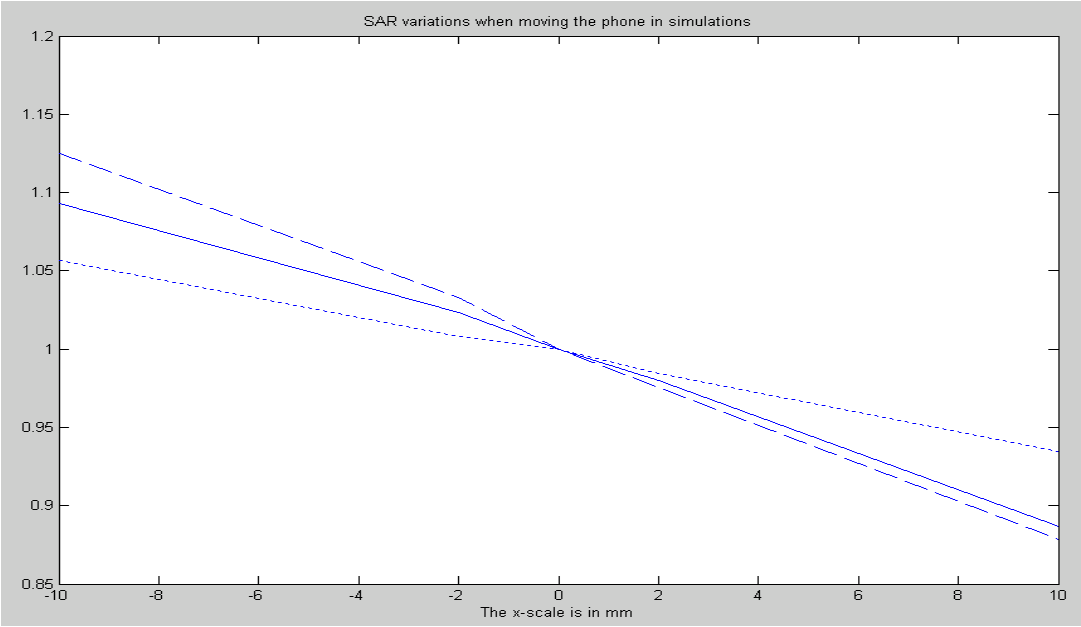

Figure 5.6, Simulations of how the SAR value depends on phone movements. The dashed line is the helical antenna placed 1 mm outwards over 1 gram; the full line is the quarter-wave whip antenna over 10 grams and the dotted line is the helical antenna placed 1 mm outwards over 10 grams. The antennas are both matched within the bandwidth 2:1 and normalised to the mid-point power level.

Comparing these results with figure 5.3 shows that the last measurement series and these simulations are quite similar. However, the simulated result seems to decrease with a rate 10 times higher than the measured results. This rate difference depends surely on that the chassis used for the simulations is just a metal box and the current distributions are not the same on the simulated surface as on the measured surface. The simulations are just done for a range of 20 mm while the measurements are done for a range of 60 mm. Because of the problems of rotating SAM, it is nearly impossible to do simulations for positions more far away than 10 mm.

The results show that when simulating a model in SEMCAD, and the position is wrong by 2-3 mm the difference in the SAR value is less than 5 % compared to the SAR value corresponding to the right position. However when the phone is moved as much as 10 mm, the SAR value varies more. Remember that for the simulations, the SAM phantom is used and for the measurements the generic twin phantom is used. Although, here it does not matter that much because the values are compared relatively. This problem is discussed in next chapter.

5.3 Comparison between the SAM phantom and the generic twin phantom

These two phantoms are available in the version of the software that was used. The simulations were mostly done with the SAM phantom and the measurements with the generic twin phantom. The generic twin model is more difficult to use and the touch position is harder to find. For that reason the SAM phantom was used for the simulations. The SAR value differs in the two models because of different shapes and different electrical parameters.

Simulations were made to compare these two cases but the outcome of these simulations is hard to interpret, due to the uncertainly in different placement configurations near the phantom head. A quarter-wave whip antenna was used on a box near the two phantoms. For the SAM phantom the SAR value over 10 grams is

1.5 W/kg. For the generic twin two simulations were done with a large difference in the outcome: the SAR values are 1.3 W/kg and 1.0 W/kg respectively. The phantom was turned 1 degree towards the phone when the lower SAR value vad computed. Also in the last simulation the phone had a larger distance to the head than in the first simulation. More investigations need to be made to say anything more about the difference of the phantoms. A problem is that the generic twin phantom is a bit clumsy to rotate and move. Only one reference point, close to the ear, is defined and the SAM phantom is easier to work with because it has here four defined reference points, and it looks more like a human head.

One solution of this problem is to simulate the SAM model with the electrical parameters for the generic twin model. This gives lower SAR values and a better comparison with measured values for the generic twin phantom. 17 simulations were done for the SAM phantom using the generic twin parameters. A factor between these two cases was calculated in Matlab. SAR value $_{\text{sam parameters}}$=k* SAR value $_{\text{generic twin parameters}}$ and k=1.087±0.008. Hence all SAR values from the simulations with the SAM phantom can be recalculated to values comparable to the measurements with the generic twin model. This is important in the next chapter where simulated cases are compared to measured cases.

The conclusions from chapter 5 are that the position of the phone is not that important regarding the SAR value. And, more important, the simulated results seem to be relatively close to the measured results, as least in theory.

6 Simulation of real cases

To check how well the program performs compared to reality, real cases are examined. However, most of the simulations in this study are compared with other simulations. From now on, the SAM phantom is used for the simulations and the generic twin phantom for the measurements.

6.1 Comparison between a quarter-wave helical antenna and a half-wave telescopic antenna

It is interesting to simulate and measure the difference of SAR values for external quarter-wave antennas compared to external half-wave antennas. In this program, it is not possible to simulate a half-wave dipole antenna and compare it with a quarter-wave antenna. Matching components are needed because the impedances are different from 50 Ω and the program does not have any features for simulating electrical components yet. A quarter-wave helical antenna can easily be matched within the 2:1 bandwidth, but a half-wave antenna has an input impedance of 300 Ω. To be able to compare these two cases a quarter-wave helical antenna is simulated (the same as in chapter 4) and compared with a half-wave telescope antenna wire put inside a quarter-wave helical antenna.

Two simulations of a phone with helical antennas are necessary as the antenna has a different distance to the head depending on if it is placed on the right or left hand side on the top of the phone. The telescope antenna is also simulated twice: once with the telescope inside the helical structure and once with the telescope outside the helical structure. There is capacitive coupling between the two elements and the whole arrangement acts as a half-wave antenna. The antenna with the telescope outside the helical antenna has theoretically the best electric characteristics but the construction is difficult to implement mechanically in an ordinary cellular phone. All simulated phones are in figure 6.1. In the figure the phantom is placed behind the phones and the face is turned to the left. All four phones are placed in the same position near the phantom. This is necessary for comparison of the results. The number of cells is equal in all four simulations and the simulation time unit is the same.

During this stage, there were problems keeping the antennas matched when placing the phone near the head. In order to avoid large mismatch errors the following procedure was used; first a pulse is simulated and then some adjustments are done and then simulations are redone. Finally, when the phone is within the 2:1 bandwidth, a simulation with a sine signal is done to compute the SAR value and the fields.

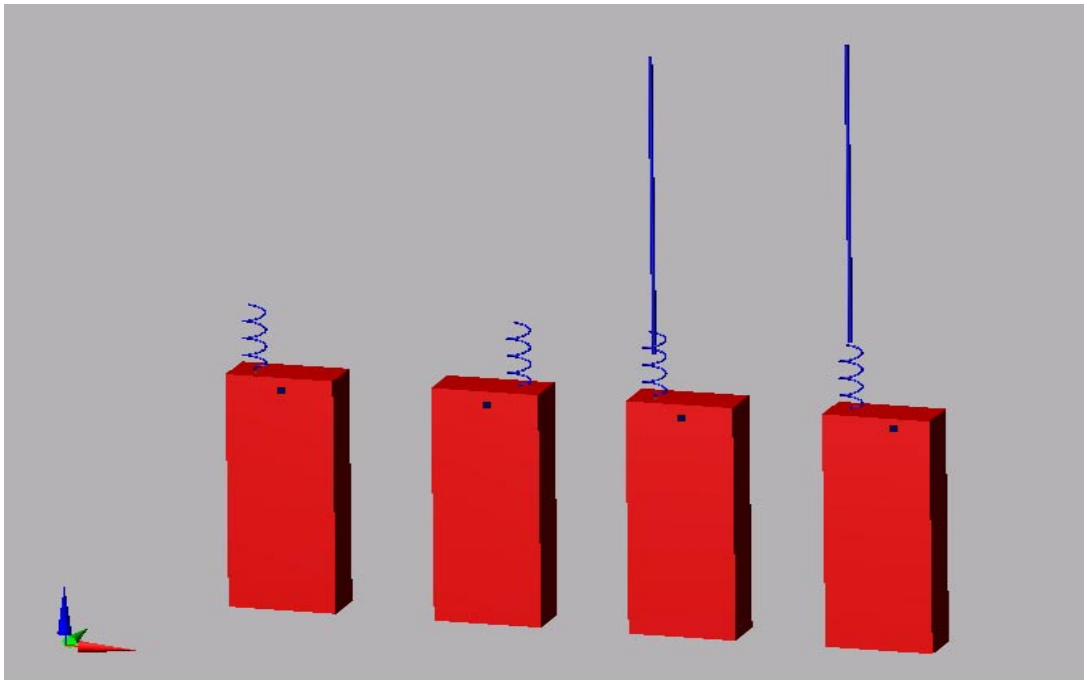

Figure 6.1, The four simulated phones. The first antenna is a helical antenna placed on the right hand side, the second is a helical antenna placed on the left hand side, the third is a telescopic antenna placed inside the helical antenna and the last is a telescope antenna placed outside the helical antenna. The point on the back is the reference point where the phone is placed near SAM.

The simulated results are in table 6.1. Here, the SAR value is higher for the antenna placed on the right hand side than for the antenna placed on the left hand side. This is because the antenna is closer to the head in the right position than in the left position. It is evident that SAR is lower for the telescope antennas than for the ordinary helical antennas. However, the SAR values for the telescope antennas are too high compared to previously known measurements, especially for the telescope antenna placed outside the helical antenna. Maybe this depends on that the coupling between the elements is not as strong here as in real antennas. The SAR values are dependent of the S11 value. If S11 is close to the band edges the SAR value is less than when S11 is in the mid-frequency.

The electric field on the surface of the phone is approximately zero for this type of half-wave antenna. When the simulated results are checked, the field is not zero on the box and as a consequence the results differ from theory. According to chapter 5.3, The SAR value can be divided by 1.08 if it is desired for generic twin parameters.

Antenna type	SAR 10g [W/kg]	SAR 1g [W/kg]	S11 [dB]
Helical antenna, right	1.57	2.92	-10.3
Helical antenna, left	1.34	2.15	-12.3
Telescope antenna, inside	0.64	1.08	-19.3
Telescope antenna, outside	1.13	2.10	-14.1

Table 6.1, SAR values from the simulations normalised to 250 mW.

Furthermore, these four antennas are simulated located 1 mm outwards from the original position near the phantom head. The results from these simulations are shown in table 6.2. The SAR values should theoretically decrease with 25 % and the results

show this. Here the problem with calculating the SAR value averaged over 1 gram occurred again. This is a bug in the system that will be fixed in future versions of SEMCAD. The SAR value for the telescope antenna inside a helical antenna is nearly the same when the phone is placed 1 mm away from the head.

Antenna type	SAR 10g [W/kg]	SAR 1g [W/kg]	S11 [dB]
Helical antenna, right	1.34	-	-12.8
Helical antenna, left	1.15	-	-14.0
Telescope antenna, inside	0.62	-	-23.2
Telescope antenna, outside	0.89	-	-22.2

Table 6.2, SAR values from the simulations when the phone is placed 1 mm outwards from the original position near the phantom, normalised to 250 mW

The time for this thesis was not sufficient to build these antennas, and compare these simulations with measurements. Instead measurements are done on the phone used in chapter 5, with four different antenna types: a helical antenna (quarter-wave), a quarter-wave whip antenna, a half-wave whip antenna and a swivel antenna (half-wave). A swivel antenna is a dipole antenna that can be turned away from the head. All antennas are single band antennas, and all measurements are made with DASY3 in the GSM band. These measurements can illustrate the difference in SAR when using a quarter-wave antenna and a half-wave antenna, see table 6.3 for the measured SAR values. Two measurements series were made and these values are average values from the two series. These values are measured with a power level 2.5 times less than the simulation power level. Hence, when comparing the measurements and simulations the measured values have to be multiplied with 2.5. See table 6.4.

Antenna type	SAR 10g [W/kg]	SAR 1g [W/kg]
Helical antenna	0.28	0.40
Whip antenna (quarter-wave)	0.47	0.66
Whip antenna (half-wave)	0.22	0.31
Swivel antenna	0.10	0.14

Table 6.3, The SAR values measured for different types of antennas with the power level set 2.5 times lower than 250 mW. Compare this table with table 6.4.

Antenna type	SAR 10g [W/kg]	SAR 1g [W/kg]
Helical antenna	0.69	1.0
Stubby antenna	1.16	1.65
Half-wave antenna	0.54	0.78
Swivel antenna	0.25	0.35

Table 6.4, The SAR values measured for different types of antennas, normalised to 250 mW.

Here, antennas with half-wave characteristics have lower SAR values than quarter-wave antennas. The swivel antenna is tilted away from the head and the maximal currents are far from the head, and as a result, it has the lowest SAR value. However,

this antenna is inconvenient to use because the antenna has to be folded every time the phone is used.

The simulated results can be compared with measurements of the Ericsson T28 phone with a retractable antenna. The PCB for this phone is smaller compared to the phone used in the simulations and it has a flex film pattern antenna with a retractable half-wave antenna. I am not allowed to discuss SAR values from commercial phones here. When the phone is used whit the antenna extended and with the telescope being used, the SAR value is less than one fifth of the original value. In the simulations the SAR value decreases with 50 % with the antenna extended.

6.2 Simulation of a patch antenna

Until now all the simulated antennas have been external antennas, such as dipole antennas or helical antennas. The antennas most often used in cellular phones today are different patch antennas. In this chapter patch antennas will be used and it will be shown how they can be simulated in SEMCAD. More information about patch antennas is in chapter 2.4.3.

Until now, all simulations have been made for 900 MHz. In order to see also how the program behaves for other frequencies, a patch antenna is simulated for 2.4 GHz. The dimensions are computed theoretically from [5], page 730, with a height of the dielectric material of 7 mm and a relative permittivity of 2.2. From these results the patch antenna is optimised in IE3D regarding the size and the feed point, and then the optimised antenna is used in SEMCAD. The matching process in SEMCAD would be very time consuming; for that reason IE3D is used for this procedure. The final dimensions of the actual patch are: 49*41 mm and for the box: 70*100*11 mm, see figure 6.2 for the model. The antenna is a half-wave antenna and as a result the dimensions are large. PML is used as boundary condition and many cells are added over the radiated structure to avoid an increasing error term from the boundary conditions and diverging simulations. The metal plane is simulated as infinitely thin with PEC. The simulation time unit is defined in seconds. The S11 for the antenna is found in figure 6.3. The antenna has a large 2:1 bandwidth, 2.37 GHz to 2.48 GHz. This depends on the size of the antenna and that the excitation mode is the half-wave length.

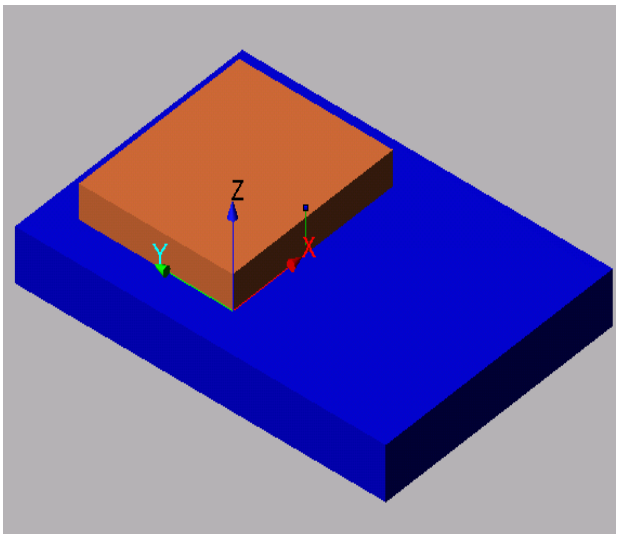

Figure 6.2, The patch antenna on a box.

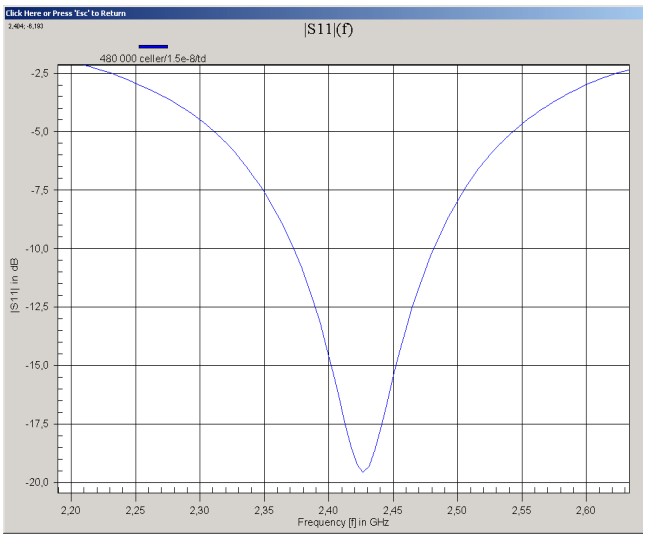

Figure 6.3, S11 for the patch antenna.

When a well-matched antenna is found, the antenna is used with a sine signal to compute the fields. This simulation with nearly 1 million cells took nearly three hours to run. The results are here presented with contour lines. In figure 6.4 the absolute E-field in the YZ plane is presented. The model is cut right through the feed point. In figure 6.5, the XZ plane is presented and in figure 6.6, the E-field in the XY plane cut on the surface of the patch is shown. The cut for the outer cells in these plots is a bit strange. This depends on that the computational area is restricted. The axes can be seen in figure 6.2.

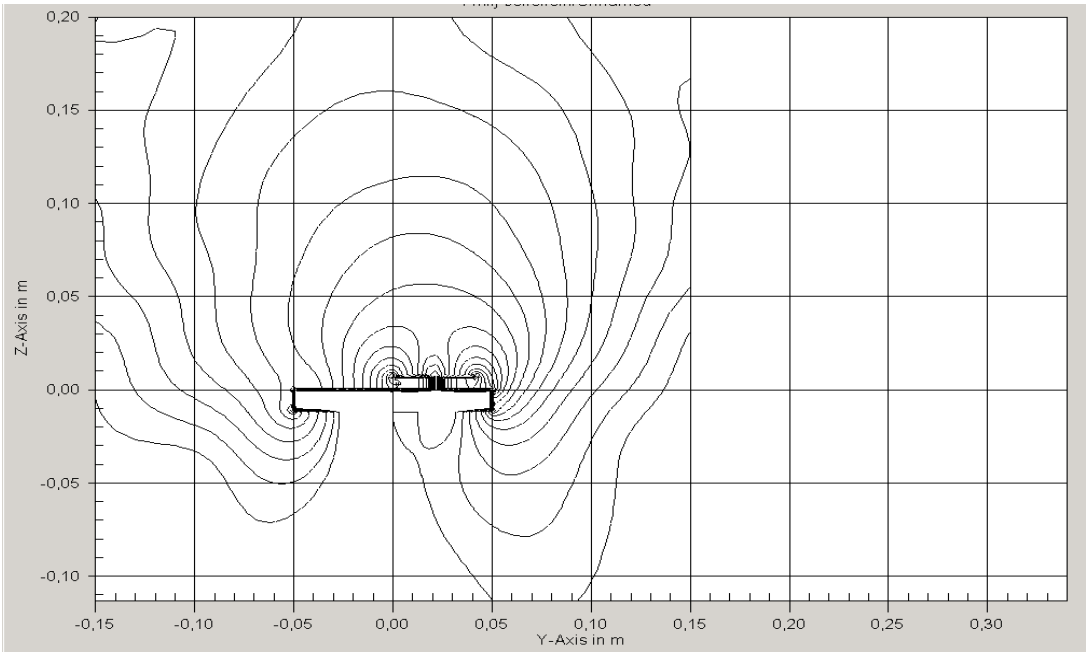

Figure 6.4, The absolute E-field cut in the X-axis at the feed point.

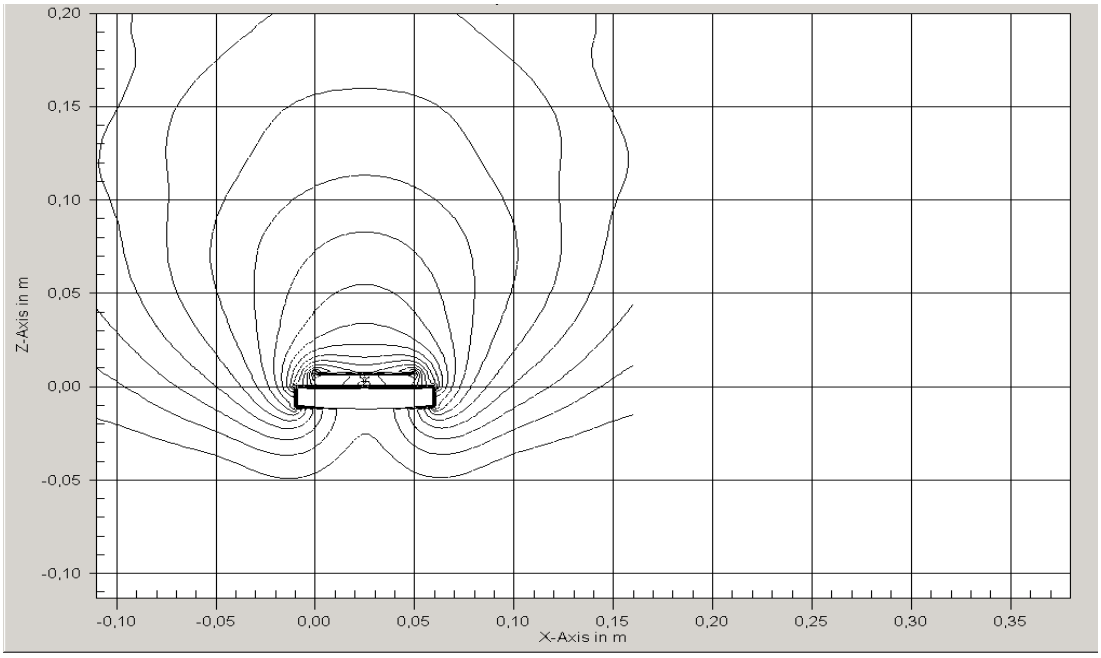

Figure 6.5, The absolute E-field cut in the Y-axis at the feed point.

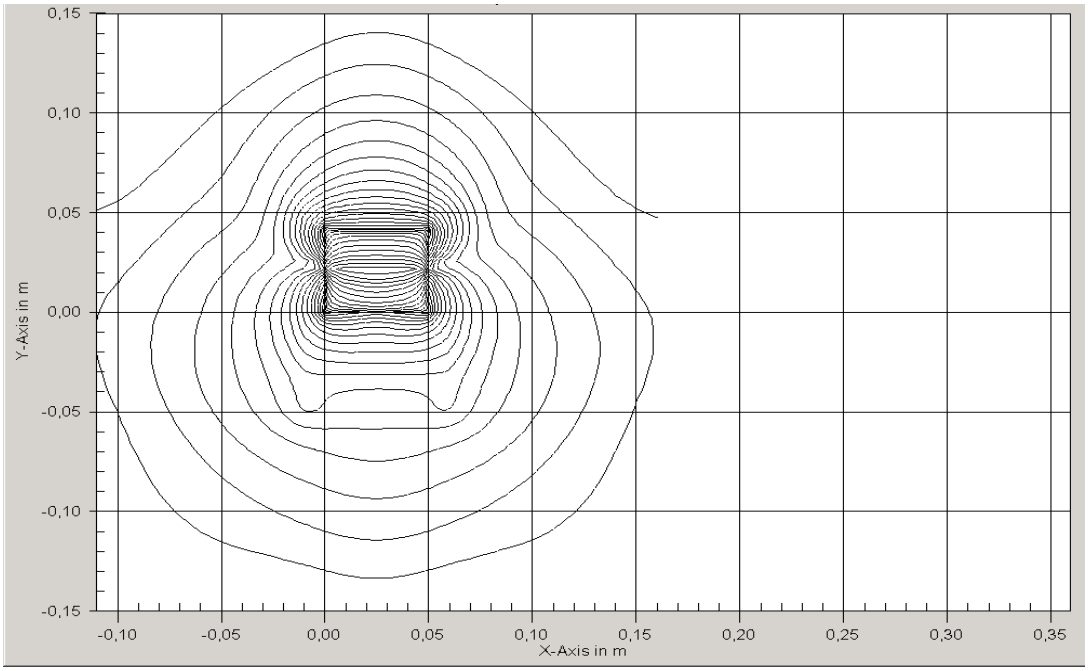

Figure 6.6, The absolute E-field cut in the Z-axis on the antenna surface.

Now this antenna will be used with SAM to simulate the SAR value near the phantom head. Problems occurred here because the phone was no longer within the 2:1 bandwidth. Many simulations were made and none of the simulations was within the bandwidth. This is due to that 2.4 GHz was used with SAM instead of 900 MHz as for GSM phones. The cells had to be a lot smaller inside the phantom than for the case with 900 MHz. The number of cells used had to be large, and when using SAM with these amounts of cells it would take a month to simulate.

If the simulations with this patch antenna had worked, it would have been interesting to take a closer look at how the SAR value changes with different placements of the feed point. The feed point can be placed either on the upper side of the patch or on the lower side of the patch. Generally problems will occur when changing the feed point because of the groundplane not being sufficiently large when the feed point is at the lower side of the patch. The feed point seems to shadow the groundplane and the antenna properties are not as good as expected. The SAR value is often large where the currents are large. If the feed point is placed on the lower part, this point is closer to the head than when it is placed in the upper part. What happens if the antenna has the feed point on the sides? In these simulations the polarisation would be different and the radiation pattern will turn 90 degrees.

6.3 Simulation of a dual band patch antenna

In order to try a real and a complex structure in SEMCAD, a dual band patch antenna was tested. First, the antenna in Nokia 8210 was simulated. See figure 6.7 for the model of this antenna. This is one of the smallest phones on the market. The antenna structure is complex, and it took over 4 days to run the simulation on nearly 7 million cells. However, this simulation turned out not to be very useful: it was diverging despite the large number of cells. The complexity of the object is large and consequently, smaller cells have to be used. PML boundary condition was used, even if it took more time to use those; the object was too small and complex. The simulation time unit was in seconds, the source was a hard source and many cells were added outside the radiating structure to avoid reflected waves; all resulting in a

large number of cells and a long computational time. In order to do this kind of a simulation within a reasonable amount of time, sub-grids are necessary.

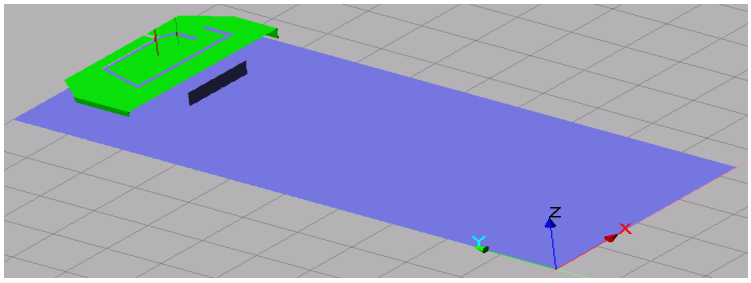

Figure 6.7, A model of the antenna in Nokia 8210

Since it is interesting to see how SEMCAD can simulate this type of antenna, a different, less complex, dual band patch antenna was chosen. This is a simple structure with two quarter-wave resonance parts, one for the DCS band (1710-1880 MHz) and the other for the GSM band (880-960 MHz), and air between the two metal sheets, see figure 6.8.

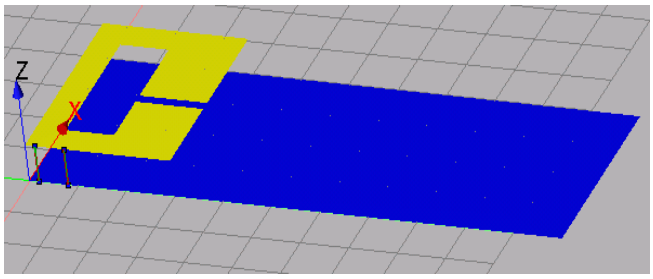

Figure 6.8, A model of a simple dual band patch antenna

This antenna was first optimised using IE3D. That took 30 minutes. Then it was simulated in SEMCAD for 11 days. The patch could not be grounded with an edge source with 0 V as shown in figure 6.8, so the simulation did not work out very well. A small metal box was used to create contact between the groundplane and the patch antenna. The simulation took nearly 12 hours and the results are shown in figure 6.9.

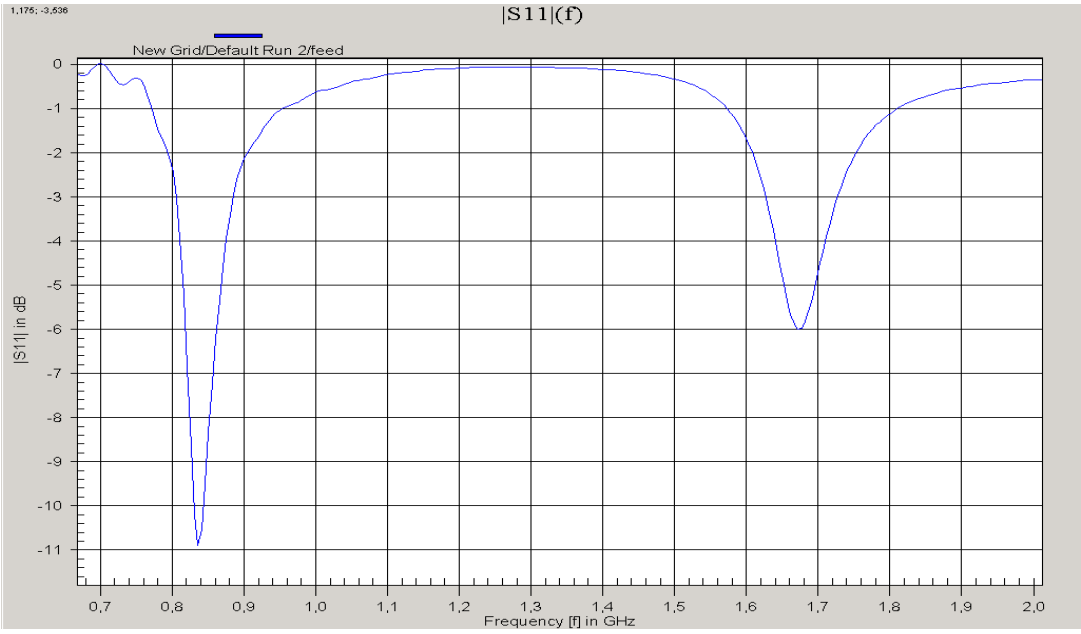

Figure 6.9, S11 for a dual band patch. The minimum step is 0.5, the maximum step is 3 and the ratio is 1.3 in every direction. The number of cells is 300 000.

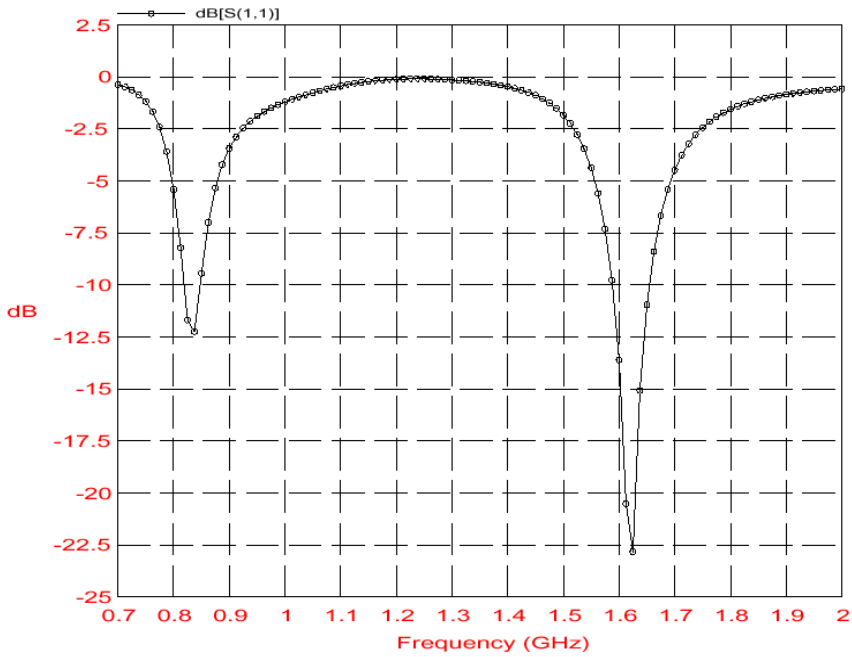

Figure 6.10, Simulated results with the same antenna from IE3D.

The antenna needs tuning for the DCS band in order to be sufficient in terms of bandwidth. A possible explanation for the frequency shift could be that the cells are sufficient for the GSM band and not for the DCS band. A simulation with smaller grids for the DCS band was run but the resonance frequency was the same.

This plot can be compared with a simulation made in IE3D for the same antenna, see figure 6.10. Please note that the scale for the Y-axis is not the same in the two figures.

The resonance frequencies for the SEMCAD simulation are about 835 MHz and 1670 MHz, for the IE3D simulation the resonance frequencies are about 840 MHz and 1620 MHz. A comparison between IE3D and SEMCAD shows that the two resonances are at the same frequency for the two programs. The return loss is nearly the same for the GSM band but for the DCS band the return loss differs. According to previous experiences, IE3D has a tendency to estimate lower return losses at high frequencies compared to reality.

To illustrate the different operating properties of the antenna at the two different resonance frequencies, the absolute total electric field is plotted for the two bands. Figure 6.11 shows the resonance for the GSM band and figure 6.12 shows the resonance for the DCS band just over the surface of the antenna.

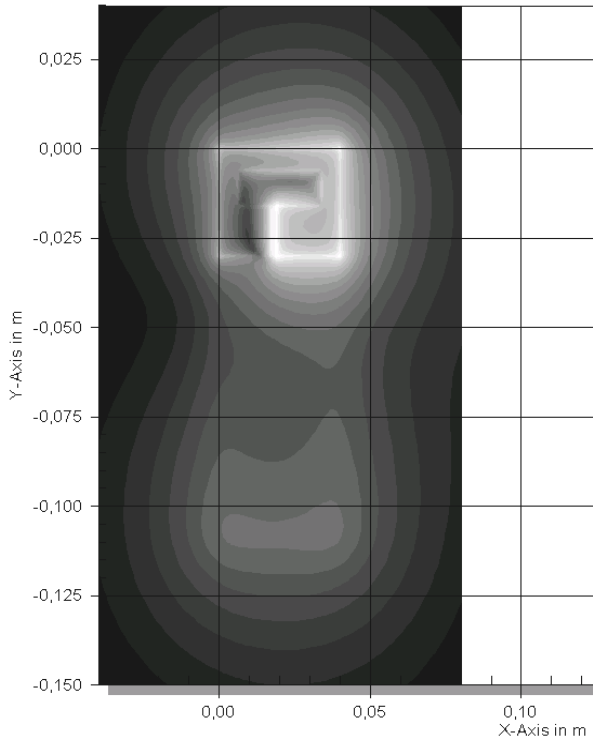

Figure 6.11, E-field for the GSM band

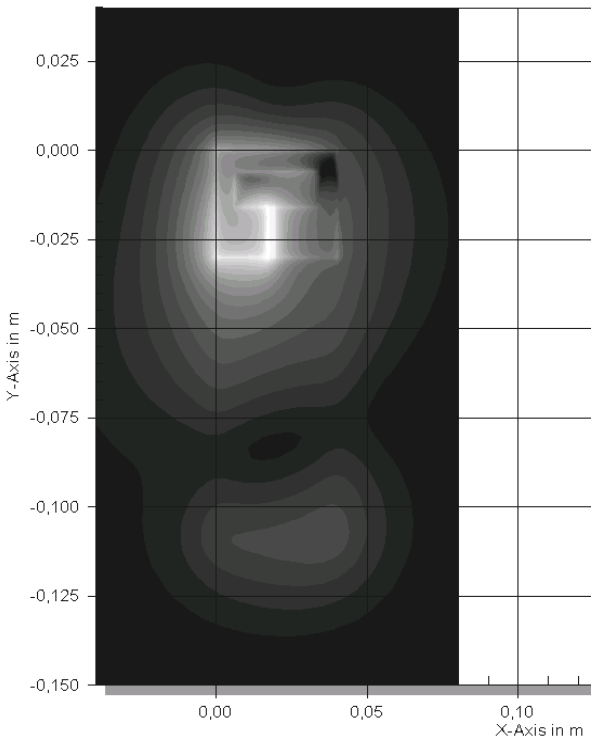

Figure 6.12, E-field for the DCS band

The dimensions of the groundplane are 110*40 mm. For GSM, the groundplane is smaller compared to the wavelength compared to the case with the DCS band. This explains why the field is larger at the groundplane in figure 6.11 than in figure 6.12. These figures also show, very clearly, which part of the antenna that is the most important in each band, the left part for the DCS and the right part for the GSM.

The results from these simulations are promising and now the phone can be run together with SAM, but this will not be done here. Modelling for a plastic cover has to be done and the time is not sufficient for that to be done.

6.4 Simulation of a real project from a CAD software package

To see how a real project from a CAD software package, in this case Pro/ENGINEER, can be implemented and simulated in SEMCAD, a complex cellular phone is imported in SEMCAD as an .STL file. Since it was impossible to import the whole object at once, the different parts were imported one at a time. This means that the object must be assembled in SEMCAD. Here the objects must be rotated and moved into the right positions. This can be tricky, but the best way is to save the project in the same co-ordinate system in CAD. When the object is imported, it cannot be edited in SEMCAD; it must be done in CAD and re-imported in SEMCAD.

The phone model cannot be shown in this thesis, but it has a complex internal patch antenna placed on a plastic carrier on a PCB. The antenna is covered with a plastic cover and a battery is placed on the cover. On the other side of the PCB, buttons and a plastic cover are placed.

A complex feed structure is used in the real phone, while in SEMCAD, the feed must be perpendicular to the original axis, therefore the feed must be redesigned in the CAD program before simulating the project. The grid is chosen to be small. The first grid evaluated has a minimum step of 0.4 and a maximum step of 3. The ratio is 1.3. Then, the baselines are edited to achieve a small structure over the antenna

surface. The number of cells is approximately 1.3 million and the simulation takes about 6 hours to run.

First the phone was simulated with and without the plastic cover for both the GSM band and the DCS band, see figure 6.14. The simulated results should theoretically show that the resonance frequency decreases when the plastic cover is used over the antenna. Here for the GSM band, the resonance frequency increases, from 980 MHz to 1100 MHz, and the resonance frequency for the DCS band decreases, from 1770 MHz to 1720 MHz. This is not correct and it was assumed that this depends on the number of cell grids or that the conductivity in the dielectric material is too high. Several simulations were done with different number of cells and conductivity parameters, but with the same results. This is a very strange behaviour that cannot be easily explained, however, this result is incorrect. Compare to the simulation of a helical antenna (figure 4.14) with a plastic cover for 900 MHz, for which the resonance frequency decreases when the plastic cover is used.

The simulations seem to oscillate for some frequencies between the interesting bands. This is because the grids are not perfect and the simulation is not long enough. But as always when simulating, the disadvantage of strange results for not relevant frequencies must be considered against longer simulation time compared to more cells and longer pulses. The interesting frequencies can be simulated each at a time with a better outcome, but here the figures shows a larger frequency range. Maybe it confuses more than explains. Simulations with energy concentrated over the interesting frequency range were run with better results for the frequencies between the two interesting frequency bands. Maybe the structure is too complex to simulate without sub-grids to obtain good, not oscillating results. This chapter shows SEMCAD's ability to handle complex problems, but it will not work completely as long as the sub-grids are not implemented.

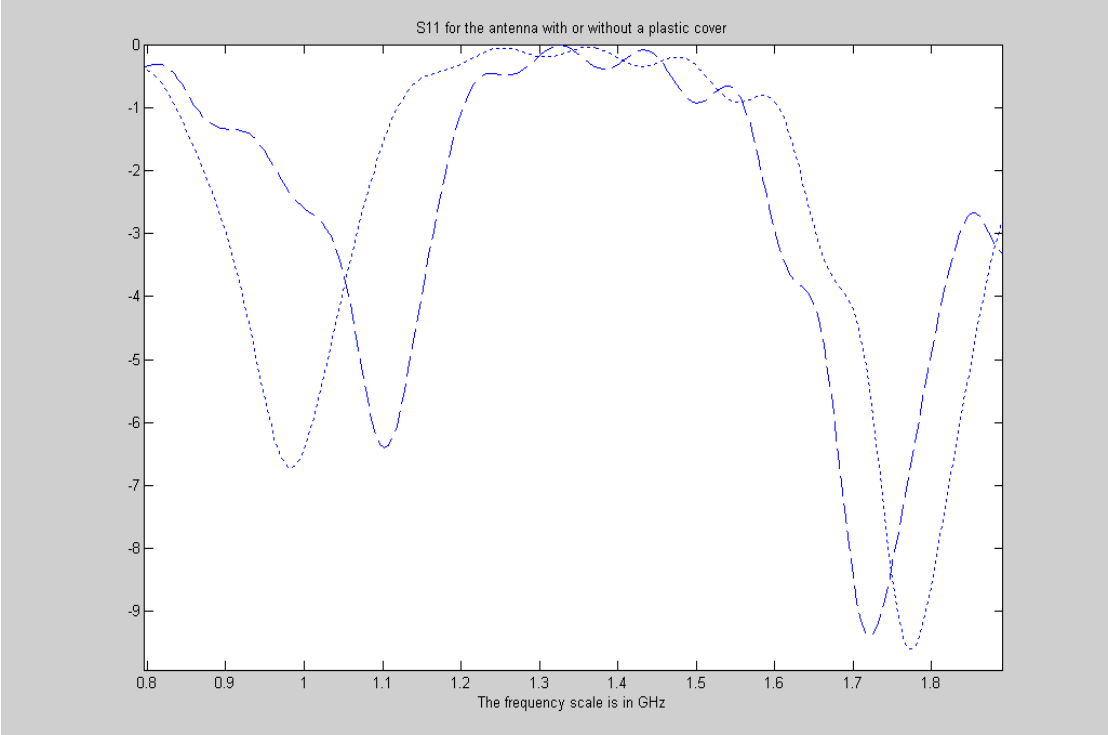

Figure 6.13, S11 for the antenna with or without a plastic cover for the GSM band and the DCS band in free space. The antenna with plastic cover is plotted with a dashed line and the antenna without the cover is plotted with a dotted line.

In figure 6.14, the antenna is measured with a network analyser with and without the plastic cover. Here, the physically correct results are shown; the resonance frequency decreases when the antenna is covered with a plastic cover. The resonance frequency for the GSM band is 1000 MHz for the antenna without a plastic cover and 960 MHz with a plastic cover. The resonance frequency for the DCS band is 1800 MHz for the antenna without a plastic cover and 1750 MHz with a plastic cover. The resonances are not sufficiently deep in S11, so the antenna should be retuned to obtain the resonance frequency in the middle of each band (GSM and DCS). This is not done here because the design process takes too much time, and there is not enough time for doing this process.

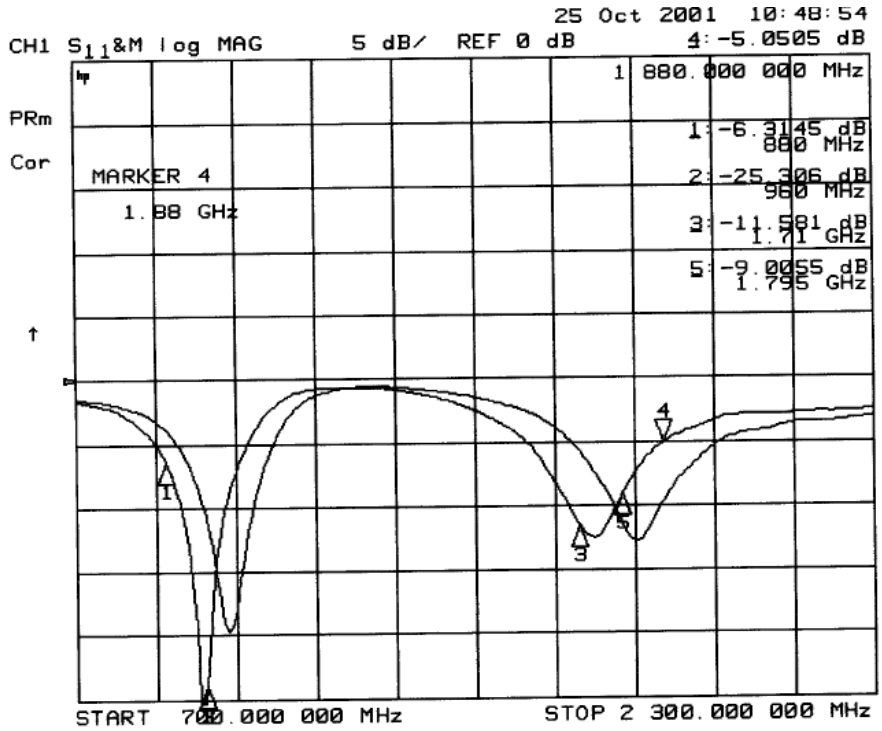

Figure 6.14, S11 measured for the antenna with or without plastic cover. The first curve is with the plastic cover and the second curve is without the plastic cover.

The two simulations with and without a plastic cover for the GSM band show an physical impossible phenomenon: the resonance frequency increases when a plastic cover is used. For the GSM band, the resonance frequency without the plastic cover seems to be quite the same. As seen in figure 6.14, the absolute value of the resonance frequency is hard to find due to the large scale used in these plots, so an error of 20 MHz must be acceptable. With the plastic cover, the GSM band has already been commented. For the DCS band, the frequency shift between using a plastic cover and not is the same in the simulations and in the measurements. However, the absolute values differ by 30 MHz, which is acceptable considering the complexity of the structure.

In figure 6.15 the phone is simulated in touch position near a phantom head for the GSM band and for the DCS band. Measurements are made for the same frequencies in talk position, see figure 6.16. The resonance frequencies are 1050 MHz and 1690 MHz for the simulations and 920 MHz and 1770 MHz for the measurements. There are larger differences in resonance frequencies for the measurements in the talk position than for the measurements in free space. This could depend on that the number of cells is not proportional to the size of the problem; more cells are needed

for the talk position simulation than for the free space simulation. Here, the simulations for both bands are done with the SAR liquid for 900 MHz, to be correct the simulations for the DCS band should be done with the SAR liquid for 1800 MHz. A simulation for the DCS band with the SAR liquid for 1800 MHz is done and no differences in resonance frequency are observable.

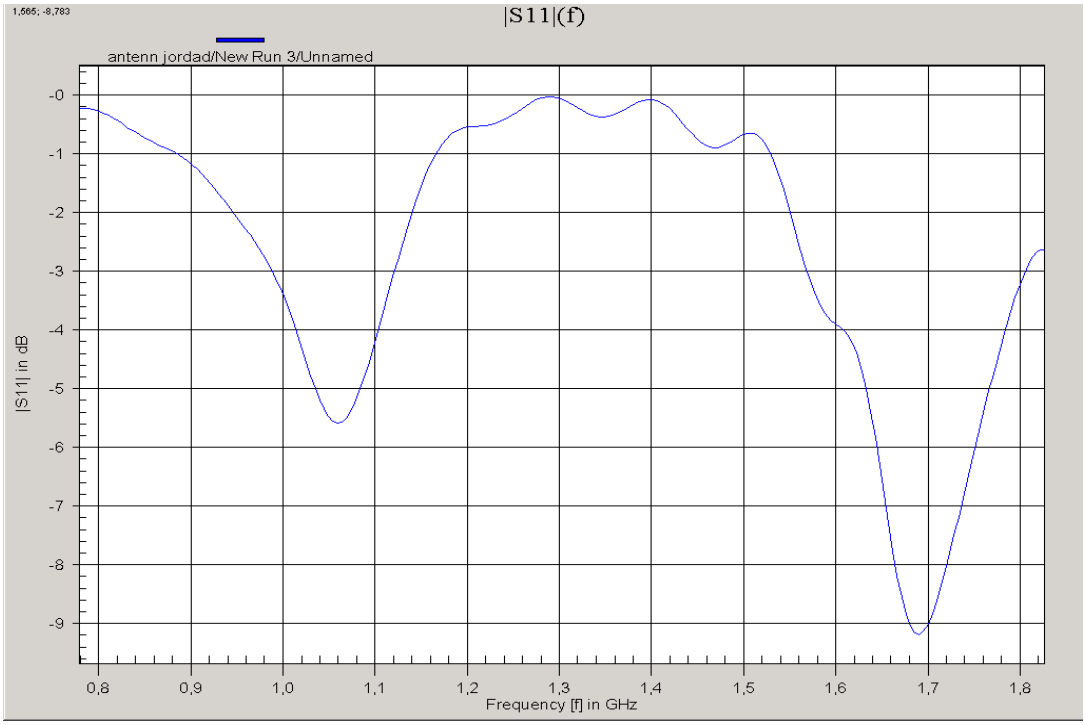

Figure 6.15, S11 simulated for the antenna with plastic cover in talk position. Here nearly 2 million cells are used.

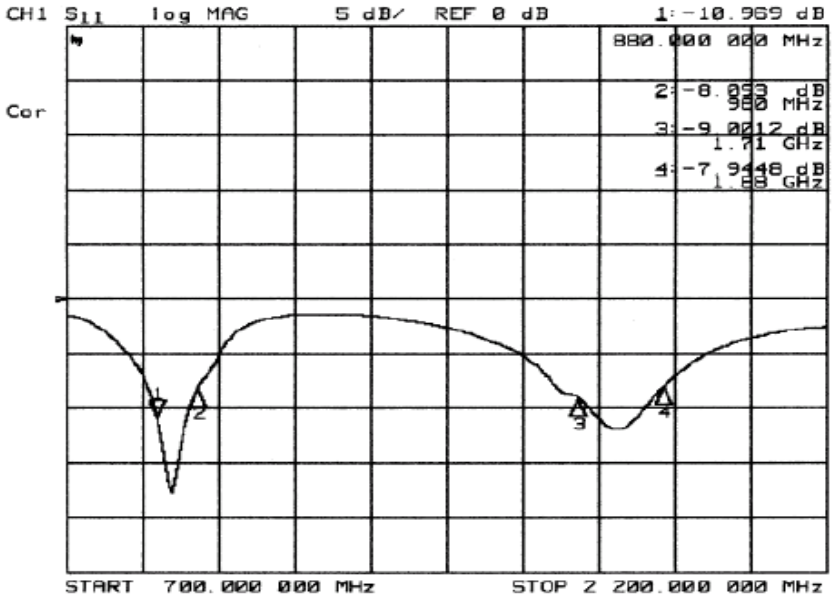

Figure 6.16, S11 measured for the antenna in talk position

The phone is now placed near the head to simulate SAR for both the GSM band and the DCS band. The plastic cover cannot be checked for the SAR computation because if checked, SEMCAD computes the SAR value inside the plastic cover too and the

only interesting SAR value is in the biological tissue. For the GSM band, the antenna had an SWR larger than 2; the SWR value was 3.2 for the resonance frequency. The SAR value was calculated to 1.34 W/kg over 10 grams and 1.89 W/kg over 1 gram. These values are possibly lower than the real values because the antenna is not transmitting enough power. For the DCS band, the antenna had an SWR less than 2 and the SAR value was 0.75 W/kg over 10 grams and 1.28 W/kg over 1 gram. These values are too high for the DCS band. The SAR value is generally lower according to measurements. It took a very long time to compute SAR with this model due to the large number of cells used for the calculations.

Measurements were done on a prototype of the phone that something could be said about these SAR values. The front plastic cover was missing and no battery was used. The measurements were instead made with a cable feeding the antenna. The distance to the phantom is hard to estimate without the plastic front; in the model the distance from the PCB to the front of the phone is 7.5 mm. The phone was placed 7.5 mm from the phantom head in the measurement set-up. Measurements were only made for the GSM band.

Problems occurred when the measurements where done because the phone was no longer matched to the mid-frequency. Measurements were made anyway. The measured SAR value was obtained as an approximate value regarding to the simulations. Three measurement attempts were completed and the phone was repositioned for each attempt. The SAR value was measured to 1.00 W/kg over 10 grams and 1.55 W/kg over 1 gram.

Here, the SAR values seem to be 30 % higher in the simulations than for the measurements. Keep in mind that the simulations are done with the SAM phantom and measurements are done with the generic twin model. The SAR value is approximately 10 % higher when measuring in the SAM phantom than in the generic twin phantom. Also, the distance from the phone to the phantom might not be the same in the two cases and as examined before; the SAR value decreases with 25 % when the phone is moved one mm from the head. The simulations were done with the SAR liquid for the SAM phantom and the measurements were done with the generic twin liquids. The electric parameters are different for these cases and simulations must be done with the same liquids in order to be able to compare these cases. Using the parameters for the generic twin phantom, the SAR value over 10 grams was 1.23 W/kg and it was 1.71 over 1 gram. These values are larger than the measured values but smaller than the values for the SAM phantom with its real parameters.

7 SAR discussion

In the world today, there are different standard committees, which have defined how the SAR value should be measured. Examples of such organisations are CENELEC, ICNIRP, ANSI-IEEE and FCC; see their homepages for more information about the different standards and the different measurement methods. The standards for the threshold value of SAR are not the same in the different organisations; they have their own phantoms and their own measurement methods. Some of them do the measurements when the phantom is holding the phone in a simulated hand and some do not. The angle of the phone towards the head is different in the different organisations. Of course, SAR depends of all these parameters. The measurements have to be made in the same way to be comparable. Some organisations considered it important to have a homogenous head phantom; some think that the phantom should be heterogeneous including every tissue of the brain in the model. One difficulty with a heterogeneous model is that it is difficult to measure and implement all the brain tissues. Another one is that people do not look the same. The complexity of a heterogeneous model is larger than the complexity of a homogeneous model. A homogenous head model is simply of a liquid with electrical parameters corresponding to the whole head for a specific frequency.

Many scientific articles produced recently are research results concerning the effects of using cellular phones. The effects of low power microwave radiation are examined, but still no proof of dangerous effects has been shown for human tissue and still the opposite has neither been proved. There are two types of effects from microwave radiation: thermal and biological. Thermal effects have been shown, but the heat increment in the brain tissue is only 0.2-0.4° Celsius, when a cellular phone is used for more than 15 minutes [11]. The increase in temperature has to be as large as 4.5° Celsius to cause permanent brain damage [11]. The temperature increase does not only come from microwave radiation; the battery in the phone is generating heat and also friction between the phone and the hand generates heat. This type of heat is different from microwave radiation, since it warms from the outside of the head, the microwaves heat from the inside of the head. The SAR limits are set very low so that no large temperature increase will occur.

What the researchers are concentrating on are the biological effects, and so far they have not found any proof of brain damages due to biological effects from microwave radiation with low power levels [12]. One type of biological effect is the ability to develop cancer. Is this risk larger when exposed to microwave radiation? Experiments on rats are done, however these experiments do not confirm any damage from microwave radiation on humans. The World Health Organisation started a project five years ago to examine the effects of exposure to electromagnetic fields. They are concentrating on the effects of short as well as long time exposure to microwaves. The effects that they are trying to find are diseases such as cancer, changes in behaviour, memory loss, Parkinson's and Alzheimer's [13]. They are planning to present the final report in 2005. The current state can be seen at their homepage, found under references.

The SAR value depends on different parameters. For example research results from Denmark [14] show that the placement of the hand is an important parameter for SAR. When the hand is held on the antenna, the SAR value in the hand is large and the radiated power is less than when the hand is not held on the antenna. The SAR limit of 4 W/kg for the hand is higher than for the head. However, in the hand no sensitive tissue like brain tissue can be damaged, and the head absorbs more power when the hand is not present so the worst-case scenario is when the hand is not

present. The hand surely absorbs more power when an internal antenna type (patch antenna) is used. When the hand is placed over the antenna most of the radiation in that direction is absorbed in the hand, so to still be able to communicate the phone increases the power level and the SAR value for the hand and the head increases too. Connection to the base station can be lost and the phone stops to work if the antenna is totally covered by the hand. The phone should be held in the hand, as far away from the antenna as possible, this is important even if using a phone with external antennas, although it is more difficult to place the hand on the antenna.

The position of the phone is essential but the most essential parameter of how the SAR value varies is the distance between the head and the phone. For a reduction of SAR the phone can be placed 1 or 2 mm away from the head. This will reduce SAR by 25 % for just one mm. Here adults have an advantage over children since adults have bigger ears and for that reason a longer natural distance from the phone to the head. The SAR value has its maximum either close to the feed point or where the phone touches the cheek.

All people are different and the SAR value is also individual for every human being, it depends on small things as, if the hair is long, if the skin is greasy, the size of the head and ear, if the persons wears glasses, if the teeth are full of amalgam, the transportation rate of blood in the head etc. It is difficult to do an accurate model for every person although the worst-case scenario is a head as large as possible, for example the soldier used in the SAM model. Tests on humans cannot be done, it is impossible to hold a cellular phone in the same position for several hours and if it is dangerous no one will do it.

SAR is always measured with full power. This power level occurs rarely when communicating, most after only during the first seconds of a phone call. The power level depends on the distance to the base station and if there are any large objects to penetrate, for example if a phone-call is made inside a building or from a train. As a result a more accurate way of measuring SAR would be both with lower power levels used when communicating and with full power. The threshold full power value could be higher than today but the low power level value should be a lot smaller than the threshold value today. The important thing to measure would be in the “talk-situation”; how much power that is used when talking in the phone.

In Sweden, a new limit for SAR is discussed. It is called the TCO standard [15]. It proposes a new of the SAR value: 0.8 W/kg over an average value of 10 grams and also it suggests a new measure called the TCP – Telephone Communication Power. This is a value of how much power that is radiating in the head when the phone is used with a power level corresponding to normal communications levels.

The best way to reduce SAR is to use a retractable antenna. The problem is that that these types of antennas are expensive to produce and they take more place inside the phone than normal antennas. Also this antenna is inconvenient because it is an external antenna and has to be extended each time you want to use the phone. This kind of antenna reduces SAR by 80 % according to measurements. However phones with internal antennas are more popular, since people care more about the disadvantage of an external antenna than radiation levels. Probably this is because of people’s lack of knowledge.

Another way to reduce SAR is to use a headset and place the phone as far away as possible from the body. In this case, the radiating antenna is far from the body and a low power level is required since no objects disturb the transmission.

8 Conclusions

First I would like to say that the program is easy to use and the modelling is easy to do. An advantage is that complex models can be imported from other CAD programs. The simulation mode is more difficult to use; the size of the cells can be chosen in many ways, the simulation parameters can also be set in many ways. It is hard to predict the outcome, so many simulations have to be redone and improved to find satisfying results.

A disadvantage of using this program is that the whole design process has to be done in SEMCAD. First the antenna has to be matched. This is when a gaussian pulse is used. Then a sine signal is used to display the fields, since the computer storage is too small to simulate the field with a gaussian pulse. The results in touch position are interesting and to compute these, the phone has to be simulated with a phantom. Perhaps the antenna is no longer matched and the matching procedure has to be redone. This takes a lot of time. Each simulation takes from 30 minutes to several hours. Surely there is other, better software that can do this process faster – for example IE3D.

The whole process does not have to be done with the matching procedure. An antenna can be matched in another program and then imported to SEMCAD for calculation of the field and simulation of SAR. The phone can also be designed in a CAD program and then imported to SEMCAD for simulations.

Today, instead of simulating, the antenna is built and then measurements are done on the antenna. Then the antenna is trimmed by hand to obtain the right properties. This process is faster than simulating and then building.

How should the simulation parameters be chosen? The grid has to be sufficiently small. This can be checked when the grid in generated. All objects have to be included and the simulated structure must correspond to the model. The simulation time has to be sufficiently large compared to other chosen parameters like frequency, source type, the variance of the pulse spectra etc. To see if the simulation has not diverged, check the voltage and current plots.

How well are simulated results compared to real measurements? The measurement series and the simulation series concerning the comparison between quarter-wave antennas and half-wave antennas varied too much. The results from simulations changed more than 10 % for 10 mm movement along the head, while the measured values were nearly constant for the changes in the placement of the phone. I did several measurements and as the SAR value did not differ a lot, more measurements are not really necessary. From all these measurements the conclusions are that if the position is moved 2-3 mm from the original defined position, the SAR variations is less than 5 %. This is in the range of normal measuring variations. Always remember here that the phone is just a model of reality.

I found it hard to use Patch antennas because the grid size and the simulation times were difficult to estimate; maybe because they were simulated for another frequency than all the other projects. There were problems when these antennas were placed near the phantom. Somehow, they were no longer within the 2:1 bandwidth. The resonance frequencies were also changing. Often the resonance frequencies were higher with SAM. I think this is because the head is a large dielectric load and also that the cells are too large compared to the object and the wavelength.

At the end of my thesis I found some interesting antennas to simulate. The complex structures have not worked before but now they did. Unfortunately the time was too short to continue simulating these antennas but the first results are interesting and useful.

Is it possible to decrease the antenna design process time by using this program? Today I will say no because the time it takes to do a matching procedure is large in SEMCAD. But as said in the introduction of this thesis, this is one of few software packages on the market that can be used for SAR estimations. If it were possible to use sub-grids the process in SEMCAD would take less time than today. SEMCAD is really a helpful tool in order to display the fields etc.

How can someone continue with the work in this thesis? Here the SAR computations were most essential, maybe someone can look more on the antenna simulations, mostly on how models from other programs can be imported and simulated. This will be easier when sub-grids are available. Another project is to simulate antennas and then build them. More measurements can be done and compared with simulations.

An important problem to solve and to work more with is why the resonance frequency increases when a plastic cover is added on the antenna. An examination of why this physical impossibility phenomenon appears should be interesting to do. Another interesting topic is a fuller investigation and comparison of the results from the SAM phantom and the generic twin. Here some simulations were done but yet there is more to investigate here.

9 References

[1] David K. Cheng, *Field and Wave Electromagnetics,* Addison and Wesley, Reading MA, 1989.
[2] Gerhard Kristensson*, Elektromagnetisk vågutbredning*, Studentlitteratur, Lund, 1999
[3] Kane S. Yee, *Numerical solution of initial boundary value problems involving Maxwell's equations in isotropic media,* IEEE Trans. Antennas Propagation, vol.14, no. 3, pp. 302-307.
[4] Allen Taflove, *Computational electrodynamics*, *The Finite-Difference Time-Domain method,* Artech house, Boston, 1995.
[5] C.A. Balanis, *Antenna theory*, John Wiley & Sons, New York, 1997.
[6] S. Gabriel, R. W. Lau and C. Gabriel, *The dielectric properties of biological tissues: III. Parametric models for dielectric spectrum of tissues*, Phys.Med. Biol. 41, pp. 2271-93, 1996.
[7] SEMCAD reference guide
[8] John D. Kraus, *Antennas*, McGraw Hill, Boston, 1998.
[9] http://www.ssi.se/nyheter/index.htm, press release the 23 February 2001, written by Gert Anger at SSI, statens strålskydds institut
[10] T. Schmid, O. Egger, N. Kuster, *Automated E-field scanning system for dosimetric assessments,* Swiss federal institute of technology, Switzerland, 1995.
[11] P. Bernardi, M. Cavagnaro, S. Pisa, E. Piuzzi, *Specific absorption rate and temperature increases in the head of a cellular phone user*, IEEE Trans. Antennas Propagation, vol.48, no. 7, pp. 1118-1126.
[12] H. Takabe, T. Shiga, M. Kato, E. Masada*, Biological and health effects from exposure to power-line frequency electromagnetic fields*, Ohmsha Ltd, Tokyo, 2001.
[13] http://www.who.int/peh-emf/publications/facts_press/swfact/sfs193.html, fact sheet number 193 from WHO.
[14] J. Graffin, N. Rots, G. Frølund Pedersen, *Radiations phantom for handheld phones*, Center for personkommunikation, Aalborg, 2000.
[15]http://www.tcodevelopment.com/s/senastenytt/tco_01/index.html?press_release.html~main, new TCO standard for measuring, press release on the 22 March 2001

Interesting Internet sites:
www.SPEAG.com, homepage for the measurement device
www.SEMCAD.com, homepage for the software
www.ssi.se/ickejoniserande_stralning/index.htm: For questions and more information in Swedish about the risks with cellular phones.
Homepages for standard organisations, for example www.fcc.gov, Federal Communications Commission in US, www.cenelec.org, Comité European de Normalisation Electrotechique, is the European organisation, www.icnirp.de, The International Commission on Non-Ionizing Radiation Protection, is a non-governmental independent organisation.
http://www.who.int/peh-emf/, WHO's homepage for the EMF project.

Appendix A, Acronyms and abbreviation

ABC	Absorbing Boundary Conditions
ANSI-IEEE	American National Standard Institute, Institute of Electrical and Electronics Engineers
CAD	Computer Aided Design
CENELEC	Comité Européen de Normalisation Electrotechique
CFL	Courant Freidrich Levy
DASY3	Dosimetric Assessment SYstem, number 3
DCS	Digital Communication System
EMC	Electro Magnetic Compatibility
EMF	Electro Magnetic Field
FCC	Federal Communications Commission
FDTD	Finite-Difference Time-Domain
GSM	Global System for Mobile communication
HPBW	Half Power Beam Width
ICNIRP	International Commission on Non-Ionizing Radiation Protection
IE3D	Integral Equation in 3 Dimensions
PC	Personal Computer
PCB	Printed Circuit Board
PEC	Perfect Electric Conductor
PMC	Perfect Magnetic Conductor
PML	Perfectly Matched Layers
RBC	Radiating Boundary Conditions
RL	Return Loss
SAM	Specific Anthropomorphic Mannequin
SAR	Specific Absorption Rate
SEMCAD	Simulation platform for EMC, Antenna Design and Dosimetry
SPEAG	Schmid & Partner Engineering AG
SWR	Standing Wave Ratio
TCO	Tjänstemännens CentralOrganisation
TCP	Telephone Communication Power
WHO	World Health Organisation